

## About an Algorithmic Approach to Tilings $\{p, q\}$ of the Hyperbolic Plane

Maurice Margenstern

(Laboratoire d'Informatique Théorique et Appliquée, EA 3097,  
Université de Metz, I.U.T. de Metz,  
Département d'Informatique,  
Île du Saulcy,  
57045 Metz Cedex, France,  
margens@sciences.univ-metz.fr)

**Abstract:** In this paper, we remind previous results about the tilings  $\{p, q\}$  of the hyperbolic plane. As proved in [Margenstern and Skordev 2003a], these tilings are combinatoric, a notion which we recall in the introduction. It turned out that in this case, most of these tilings also have the interesting property that the language of the splitting associated to the tiling is regular. In this paper, we investigate the consequence of the regularity of the language by providing algorithms to compute the path from a tile to the root of the spanning tree as well as to compute the coordinates of the neighbouring tiles. These algorithms are linear in the coordinate of the given node.

**Key Words:** discrete hyperbolic geometry, combinatorial approach, tilings

**Category:** F.2.2

### 1 Introduction

Hyperbolic geometry appeared in early nineteens after a long search for proving the famous parallel postulate from the other postulates of Euclid's geometry. It appeared that the famous axiom could not be proved from the others because a new geometry could be built on these axioms together with a negation of the parallel axiom. This new geometry independently built by Lobachevsky and Bolyai assumes that in the plane, at least two distinct parallels to a given line pass through a given point not lying on the line. A bit later, models were found for the new geometry by Beltrami, then Klein, then Poincaré and many others. Here, we shall use Poincaré's disc model, today the most popular.

It follows from the well-known Poincaré's theorem, that for any positive numbers  $p$  and  $q$  such that  $\frac{1}{p} + \frac{1}{q} < \frac{1}{2}$ , there is a tiling of  $\mathbb{H}^2$  by replicas of the regular polygon with  $p$  sides and with  $\frac{2\pi}{q}$  as the interior angle between consecutive sides. Traditionally, these tilings are denoted by  $\{p, q\}$ . In this paper, we remember the proof that all these tilings are **combinatoric**, a notion which we explain below. We also prove again that the language of the splitting attached to combinatoric tilings turns out here to be regular. Opposite to the case of the

pentagrid where good algorithms are a straightforward corollary of the regularity of the language, here also we have good algorithms, but the property is far from being an easy consequence of the regularity of the language attached to the splitting. The reason can be explained in this way. In the pentagrid, there is no difference between the notion of generation of a level of nodes in the tree and the notion of generation by the recursive reflection of image polygons in their sides. In the general case of the tilings  $\{p, q\}$ , there is a difference. As we shall see in section 3, a new level in the tree gives access to several generations in the reflection process. But it is not uniformly the same number of generations which is accessed at each generation of a level. And so, we have a choice: either to proceed according to the reflection process or to proceed according to the tree process. We shall see that in the tree process, it is possible to have linear algorithms to compute the path from a node of the tree to the root and to compute the coordinates of the neighbours of the node. The algorithms are linear in time and in space in the coordinate of the considered node. In this paper, I consider the tree process, the reflection process being the goal of another paper with G. Skordev.

Below, in section 1, we briefly remember the basic features of hyperbolic geometry. Then, in section 2, we explain the splitting method, which is at the basis of the results of this paper, explaining its main features on the example of a particular case of the tilings  $\{p, q\}$ : the case of  $\{5, 4\}$ , now called the **pentagrid** which is constructed by reflection from the regular rectangular pentagon. In section 3 we indicate the splitting of  $\mathbb{H}^2$  giving rise to the tiling  $\{p, q\}$ , remembering the results obtained for the matrix and the polynomial of the splitting. In section 4, we describe the tools which are needed to define the algorithms which are given in section 5 together with the analysis of their complexity.

## 2 Hyperbolic geometry

As mentioned in the introduction, Poincaré's disc model is probably the most popular model of the hyperbolic plane.

In Poincaré's disc model, the hyperbolic plane is the set of points which lie in the open unit disc of the Euclidean plane. The lines of the hyperbolic plane are represented either by diametral segments (open segments as the points lying on the unit circle do not belong to the hyperbolic plane) or trace in the open disc of circles which are orthogonal to the unit circle. We shall say that the considered circle **supports** the hyperbolic line. Later we shall say ***h*-line** for hyperbolic line, and most often simply **line** when there is no ambiguity.

The points which are on the unit circle do not belong to the hyperbolic plane. However, we call them **points at infinity** for obvious topological reasons. It is not difficult to see that a line has exactly two points at infinity and, conversely

two distinct points, either in the plane or at infinity, define a unique line passing through them. As shown by figure 1 below, there are three cases for the intersection of two lines in the model: either the intersection is empty, and then we say that the lines are **non-secant**; or the intersection consists of exactly one point. If this point is in the plane, we say that the lines are **secant** and that they meet in this point; if the point is at infinity, we say that the lines are **parallel**. Figure 1 shows that there are exactly two parallels to a given line through a point which does not lie on the line.

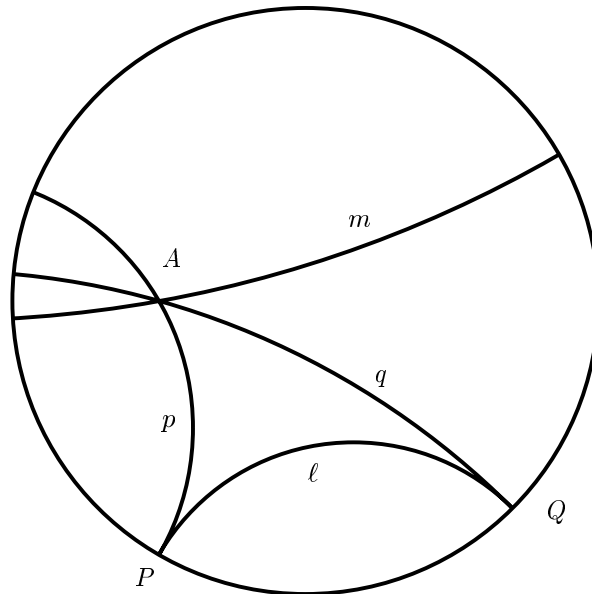


**Figure 1** The lines  $p$  and  $q$  are parallel to the line  $\ell$ , with points at infinity  $P$  and  $Q$ . The line  $m$  is non-secant with  $\ell$ .

The main reason for choosing this model lies in its definition of the angles. The angle between two  $h$ -lines is defined as the Euclidean angle between the tangents to the circles which support these  $h$ -lines. In particular, orthogonal circles support perpendicular  $h$ -lines.

Another aspect of the parallel axiom lies in the sum of the interior angles at the vertices of a polygon. In the Euclidean plane, the sum of the angles of any triangle is exactly  $\pi$ . In the hyperbolic plane, this is no more true: the sum of the angles of a triangle is **always less** than  $\pi$ . The difference from  $\pi$  is, by definition, the **area** of the triangle in the hyperbolic plane. Indeed, one can see that the difference of the sum of the angles of a triangle from  $\pi$  has the additive

property of a measure on the set of all triangles. As a consequence, there is no rectangle in the hyperbolic plane. Consequently two non-secant lines, say  $\ell$  and  $m$ , have, at most, one common perpendicular. It can be proved that this is the case: two non-secant lines of the hyperbolic plane have exactly one common perpendicular, see for instance [Meschkowski 1964]. Indeed, this property is a characterization of the property for lines to be non-secant. It is not difficult to prove that secant or parallel lines have no common perpendicular.

Another deep difference between Euclidean and hyperbolic geometries is that in the former we have the notion of **similarity**: in the Euclidean plane, there are infinitely many triangles with the same interior angles and with different sizes. This is no more true in hyperbolic geometry: given  $\alpha, \beta$  and  $\gamma$  with  $\alpha + \beta + \gamma < 1$ , all the triangles of the hyperbolic plane with the angles  $\alpha, \beta$  and  $\gamma$  are isomorphic.

However, there is an important tool which can be used in both planes: the notion of **reflection** in a line. It is defined as follows in the disc model of  $\mathbb{H}^2$ . Let  $\ell$  be a  $h$ -line and let  $\Omega$  be the centre of the Euclidean circle which supports  $\ell$  and let  $R$  be its radius. Two points  $M$  and  $M'$  are **symmetric** with respect to  $\ell$  if and only if  $\Omega, M$  and  $M'$  belong to the same Euclidean line and if we have  $\Omega M \cdot \Omega M' = R^2$ . Moreover,  $M$  and  $M'$  do not lie in the same connected component of the complement of  $\ell$  in the unit disc. We also say that  $M'$  is obtained from  $M$  by the reflection in  $\ell$ . It is clear that  $M$  is obtained from  $M'$  by the same reflection. In elementary geometry, this transformation of  $M$  into  $M'$  is called **inversion** of  $M$  with respect to  $\ell$ .

All the transformations of the hyperbolic plane which we shall later consider are reflections or constructed by reflections.

It can be proved that for any couple of two lines  $\ell$  and  $m$ , there is a line  $n$  such that  $\ell$  and  $m$  are exchanged by the reflection in  $n$ . In the case when  $\ell$  and  $m$  are non-secant,  $n$  is the perpendicular bisector of the segment which joins the intersections of  $\ell$  and  $m$  with their common perpendicular.

## 2.1 Tessellations in hyperbolic spaces

Tessellations in the plane – the definition is independent of the geometry which we consider – consist in the following operations. First, take a convex polygon  $P$ . Let  $\mathcal{S}(P)$  be the set of the lines which support its sides. If  $\mathcal{E}$  is a set of polygons, one extends  $\mathcal{S}$  to  $\mathcal{E}$  by setting  $\mathcal{S}(\mathcal{E}) = \bigcup_{P \in \mathcal{E}} \mathcal{S}(P)$ . Given  $\mathcal{K}$  a set of lines and  $\mathcal{E}$  a set of polygons, we define  $\rho_{\mathcal{K}}(\mathcal{E}) = \bigcup_{k \in \mathcal{K}, Q \in \mathcal{E}} \rho_k(Q)$ . Setting  $\mathcal{T}_0 = \{P\}$ , we inductively define  $\mathcal{T}_{k+1}$  by  $\mathcal{T}_{k+1} = \rho_{\mathcal{S}(\mathcal{T}_k)}(\mathcal{T}_k)$ . Finally, we define  $\mathcal{T}^* = \bigcup_{k=0}^{\infty} \mathcal{T}_k$  to be the **tessellation** generated by  $P$ . We say that the tessellation is a **tiling** if and only if any point of the plane belongs to at least one polygon in  $\mathcal{T}^*$  and if the interiors of the elements of  $\mathcal{T}^*$  are pairwise disjoint.

In this definition, the lines are defined according to the considered geometry. It may have a consequence on the existence of a tessellation, depending on which polygon is taken in the first step of the construction. As an example, starting from a regular figure, there are basically three possible tessellations giving rise to a tiling of the Euclidean plane: the three regular tilings which are based on the square, the regular hexagon and the equilateral triangle.

We can now state the theorem:

**Theorem 1, Poincaré's Theorem**, ([Poincaré 1882]) – *Any triangle with the interior angles  $\pi/\ell, \pi/m, \pi/n$  such that*

$$\frac{1}{\ell} + \frac{1}{m} + \frac{1}{n} < 1$$

*generates a unique tiling by tessellation.*

As an immediate corollary of the theorem, tilings based on any regular polygon with  $p$  sides and interior angle  $\frac{2\pi}{q}$  do exist, provided that  $\frac{1}{p} + \frac{1}{q} < \frac{1}{2}$ . Such a polygon and the corresponding tiling are denoted by  $\{p, q\}$ .

### 3 The splitting method: a combinatorial approach

The splitting method was first defined in two papers: in [Margenstern 2002a] and in [Margenstern 2003a]. The definition runs as follows:

**Definition 1** *Let  $S_0, \dots, S_k$  be finitely many parts of some geometric metric space  $X$  which are supposed to be closed with non-empty interior, unbounded and simply connected. Let  $P_1, \dots, P_h$  with  $h \leq k$  be finitely many closed simply connected bounded sets. Say that the  $S_i$ 's and  $P_\ell$ 's constitute a **basis of splitting** if and only if:*

- (i)  $X$  splits into finitely many copies of  $S_0$ ,
- (ii) any  $S_i$  splits into one copy of some  $P_\ell$ , the **leading tile** of  $S_i$ , and finitely many copies of  $S_j$ 's,

where **copy** means an **isometric image**, and where, in the condition (ii), the copies may be of different  $S_j$ 's,  $S_i$  possibly included.

As usual, it is assumed that the interiors of the copies of  $P_\ell$  and the copies of the  $S_j$ 's are pairwise disjoint.

The set  $S_0$  is called the **head** of the basis and the  $P_\ell$ 's are called the **generating tiles** and the  $S_i$ 's are called the **regions** of the splitting.

Say that a tiling of  $X$  is **combinatoric** if  $X$  has a basis of splitting and if the spanning tree of the splitting yields exactly the restriction of the tiling to  $S_0$ , the head of the basis.

Consider a basis of splitting of  $X$ , if any. We recursively define a tree  $A$  which is associated with the basis as follows. The **root** of  $A$  is the leading tile of  $S_0$ . Consider the region  $S_i$  associated to the considered node, say  $\nu$ . Splitting  $S_i$  according to the condition (ii) of the above definition, we take the leading tiles of the regions which are obtained as the sons of  $\nu$ . This defines an infinite tree  $A$  with finite branching which we call the **spanning tree of the splitting**, where *splitting* refers to the basis of splitting, with its regions  $S_0, \dots, S_k$  and its generating tiles  $P_0, \dots, P_h$ .

The fact that the hyperbolic plane is able to embed infinite trees is not new. This is already known from Gromov's works, see [De la Harpe et al. 1990] for instance, which points at the tree structure as the key structure of a hyperbolic space. However, before [Margenstern and Morita 2001], which exhibits the tree in a *natural* way, no *application* of that idea was done.

This is what we see in the first sub-section by proving that the pentagrid is combinatoric. In the second sub-section, we shall see the algebraic consequences of the definition.

### 3.1 The classical example of splitting: the pentagrid

As already indicated, the **pentagrid** is defined as the tessellation  $\{5, 4\}$  of the hyperbolic plane, *i.e.*, the tiling defined by the reflections of the regular rectangular pentagon in its sides and, recursively, of the images in their sides, see figure 2.

The existence of the pentagrid is a direct consequence of Poincaré's theorem: suitably displayed, ten copies of the hyperbolic triangle with the angles  $\frac{\pi}{4}$ ,  $\frac{\pi}{2}$  and  $\frac{\pi}{5}$  constitute a regular pentagon with right angles.

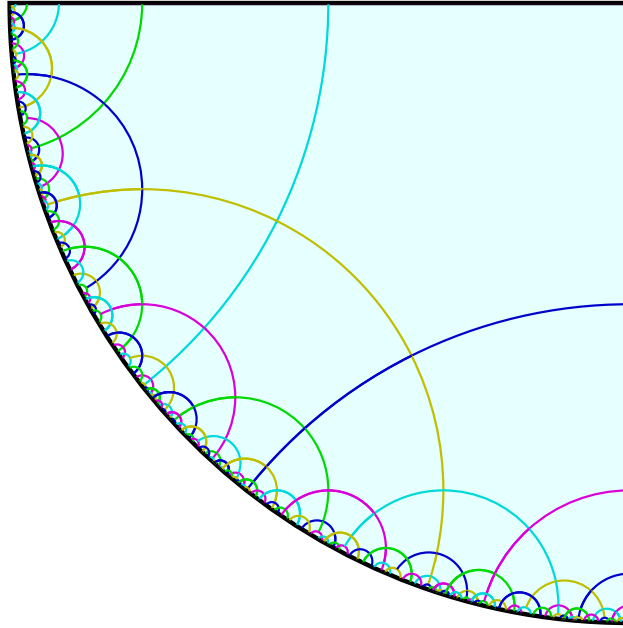


**Figure 2** *The pentagrid in the south-western quarter.*

Consider figures 3 and 4, below. They represent a restriction of the pentagrid to a quarter  $Q$  of  $\mathbb{H}^2$  which we represent by the south-western quarter of the unit disc. We place a tile  $P_0$  with a vertex in  $O$  and two sides on the borders of the quarter. Note that  $R_1$ , delimited by the support of the sides **1** and **2** is the image of  $Q$  by the shift along **1** transforming **5** into **2**. Similarly,  $R_2$ , delimited by the sides **2** and **3** is the image of  $Q$  under the shift along **4** transforming **5** into **3**. Now, denote by  $R_3$  the closure of the complement in  $Q$  of  $P_0 \cup R_1 \cup R_2$  and call it a **strip**. Say that we split the quarter  $Q$  in  $P_0$ , which we call its **leading pentagon**, and the regions  $R_1$ ,  $R_2$  and  $R_3$ .

By recursion, we can now repeat this splitting in any region which is an isometric image of  $Q$ .

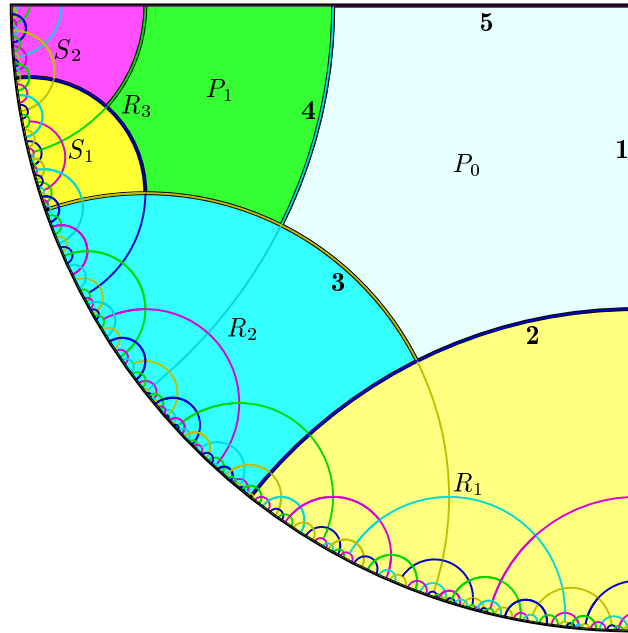


**Figure 3** *Splitting the quarter into four parts*

*First step: the regions  $P_0$ ,  $R_1$ ,  $R_2$  and  $R_3$ , where the region  $R_3$  is constituted of the regions  $P_1$ ,  $S_1$  and  $S_2$ ;*

*Second step: the regions  $R_1$  and  $R_2$  are split as the quarter (not represented) while the region  $R_3$  is split into three parts:  $P_1$ ,  $S_1$  and  $S_2$  as indicated in the figure.*

Now, consider the strip. It is what we obtain from a quarter when we remove from it another quarter delimited by the leading tile. Indeed, let  $U$  be the image of  $Q$  under a shift  $\tau$  along the side **5**. Then  $R_3 = U \setminus R_2 = U \setminus (U \cap R_2)$  and it is not difficult to see that  $U \cap R_2$  is a quarter. Note that  $U \setminus R_2$  is the image of  $Q \setminus R_1$  under  $\tau$ . Now, the strip contains a pentagon,  $P_1$ , see figures 3 and 4, and the complement of  $P_1$  in  $R_3$  contains an isometric image of  $Q$ : it is denoted by  $S_1$  in figures 3 and 4. Indeed, an appropriate shift along the side **3** of  $P_0$  transforms  $R_2$  into a region which is the reflection of  $S_1$  in the line which supports the side **3** of  $P_0$ . It is not difficult to obtain  $S_1$  by a shift from  $Q$ :  $S_1$  is the image of  $U$  under a shift along the side of  $P_1$  which is adjacent to line **5** and which is opposite to **4**, the common side of  $P_0$  and  $P_1$ .

Now, it is not difficult to note that the closure of the complement in  $R_3$  of  $P_1 \cup S_1$ , call it  $S_2$ , is again a strip: it is the image of  $R_3$  under  $\tau$  again.

Now, we can repeat the splitting of any region which is an isometric image of the strip  $R_3$ .

As indicated above and illustrated by figure 4, now we can construct a tree  $\mathcal{A}$



whose nodes are associated to the leading pentagons of the regions which are defined by the recursive splitting of the already obtained regions.

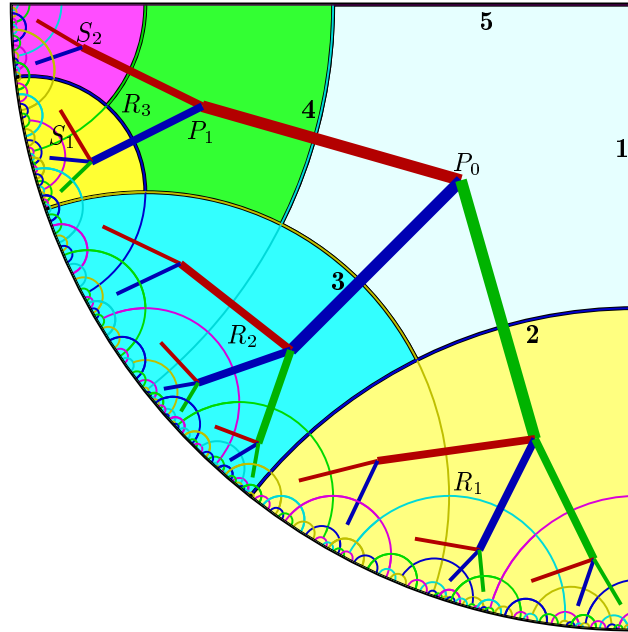


**Figure 4** *Splitting a quarter and a strip: with the help of the generated tree.*

As illustrated in figure 4, there are two kind of nodes in  $\mathcal{A}$ , depending on whether the region which is associated with the corresponding leading pentagon is a copy of a quarter or of a strip. In the case of a copy of a quarter, we say that we have a **white** node. We also say a 3-node because it has three sons. In the case of a copy of a strip, we say that we have a **black** node. We also say a 2-node because it has two sons. Another representation of the tree is given by figure 5 below, where another information is also displayed.

### 3.2 Algebraic consequences: the classical example of the pentagrid

In the general case, when a tiling is combinatoric, we represent the splitting of the regions of the basis by an **incidence** matrix which we call the **matrix of the splitting**. Each row  $i$  is associated to a region  $S_{i-1}$  and, on each column  $j$ , we have how many copies of  $S_{j-1}$  enter the splitting of  $S_{i-1}$  according to the condition (ii) of the definition. Now, when we have a square matrix  $M$ , we can attach to it its characteristic polynomial  $P$ . When  $M$  is the matrix of a splitting of a combinatorial tiling, we call **polynomial of the splitting** the just defined polynomial  $P$  possibly divided by the greatest power of  $X$  which it contains.

Next, a new ingredient comes, which was first used in [Margenstern 2001]. Let us see what happens in the case of the pentagrid.

Number the nodes of the spanning tree: 1 is given to the root and the following numbers to the next nodes, level by level and, on each level from the left to the right. Easy computations show that the number  $u_n$  of nodes of the spanning tree at the level  $n$ , the root being at the level 0, is  $f_{2n+1}$ , where  $f_n$  is the Fibonacci sequence fixed by  $f_0 = 1$  and  $f_1 = 1$ .

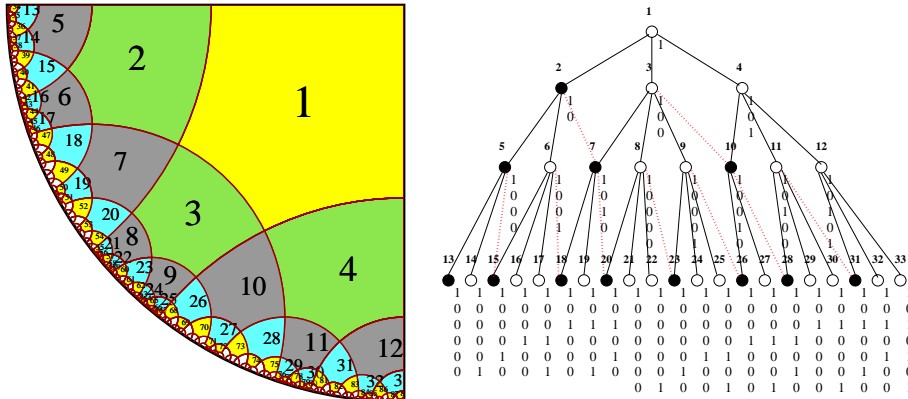


**Figure 5** *Numbering the nodes of the spanning tree. On the right-hand side: the property of the maximal Fibonacci representation.*

This is why in [Margenstern 2001] I considered the representation of the numbers of the nodes in the basis of the just mentioned Fibonacci sequence  $\{f_i\}_{i>0}$ . It is known that this representation is not unique but it can be made unique by fixing the condition: 11 is ruled out from the representation. We get the so-called maximal Fibonacci representation which, later on, we call the **coordinate** of the considered node.

Let  $\alpha_k \dots \alpha_0$  be the coordinate of the node with number  $n$ . We call **continuator** of  $n$  the node whose coordinate is  $\alpha_k \dots \alpha_0 00$ . Accordingly, a node will be called a **continuator** if it is the continuator of some node.

We obtain a very interesting property, first proved in [Margenstern 2001]:

**Theorem 2** ([Margenstern 2001]) – *For each node of the spanning tree of the tiling  $\{5, 4\}$ , its continuator occurs among its sons and there is no other continuators among its sons.*

The property is proved in [Margenstern 2001] to which we refer the interested reader. Later on, we call **preferred son property** the property stated in theorem 2.

We remark that this property is in tight connexion with the well known property that the set of coordinates of the spanning tree constitutes a regular language over  $\{0, 1\}^*$ .

Coming back to the general case, we can perform a similar numbering of the nodes of the spanning tree. Then, it turns out that in all cases which we studied, the polynomial of the splitting has a positive greatest real root  $\beta$ , with  $\beta > 1$ . Then, it is possible to represent the positive numbers in the basis of the sequence  $u_n$  which we defined above and which observes the linear recurrent relation defined by the polynomial of the splitting. It is known, see [Fraenkel 1985, Hollander 1998], that any positive number  $n$  can be written as  $n = \sum_{i=1}^k \alpha_i u_i$ , where  $\alpha_i \in \{0..b\}$ , with  $b = \lfloor \beta \rfloor$ . In general, this representation is not unique, but here also, it can be made unique by choosing the maximal representation with respect to the lexicographic order on  $\{0..b\}^*$ . We also call **coordinate** of node  $\nu$  the maximal representation of the number attached to it in basis  $\{u_n\}_{n>0}$ . We call **language of the splitting** the language of the coordinates of the nodes of the spanning tree of the splitting.

Many tilings of the hyperbolic plane turn out to be combinatoric with a regular language of the splitting. There are detailed proofs for the tilings  $\{p, 4\}$  and  $\{p, 3\}$ . See [Margenstern and Skordev 2003b] and [Margenstern et al. 2004b] for, respectively  $\{p, 4\}$  and  $\{p, 3\}$ . In [Margenstern et al. 2004b], an interesting connection is established between both families of tilings: the spanning trees of the splitting of  $\{p, 4\}$  and  $\{p+2, 3\}$  are the same. There are also combinatoric tilings for which the language of the splitting is not regular: most cases of the triangular tessellations, see [Margenstern 2003c], a tiling of the hyperbolic 3D space, see [Margenstern and Skordev 2003c], and a tiling of the hyperbolic 4D space, see [Margenstern 2004].

#### 4 The regular grids $\{p, q\}$

Now, we turn to the regular grids  $\{p, q\}$  which we defined in our introduction. From the condition  $\frac{1}{p} + \frac{1}{q} < \frac{1}{2}$ , we can see that the smallest value of  $q$  is 3 and, in that case,  $p \geq 7$ . Symmetrically, the smallest value of  $p$  is 3 and, in that case,  $q \geq 7$ .

As above indicated, the particular cases  $q = 4$  and  $q = 3$  are already fixed in previous papers.

We shall see that in the other cases, the splitting method can always be applied too. It also appears that the tilings are combinatoric and that the language of the splitting is always regular. However, except the important case of the tilings  $\{p, 3\}$  and  $\{p, 4\}$ , the splitting does not match the group approach

definition of generation. In the general case, a generation according to the spanning tree of the splitting contains several generations defined by reflection in sides. However, we have rather simple algorithms provided by a refinement of our combinatoric approach.

#### 4.1 Splitting a tiling $\{p, q\}$

We remember the following result:

**Theorem 3** (Margenstern, Skordev [Margenstern and Skordev 2003a]) – *The tilings  $\{p, q\}$  are combinatoric and the language of the splittings is regular when  $p \geq 4$ .*

Note that this is the best result: as proved in [Margenstern 2003c], the language of the splitting is not regular for the tilings  $\{3, q\}$ , the case of equilateral triangles.

As later we need a precise information in the way in which we perform the splitting, we repeat here the proof already given. This is also for completeness, for the reader's convenience.

It is well known that in hyperbolic geometry, several properties of the group of symmetries of the regular polygons with  $p$  sides and an angle vertex of  $\frac{2\pi}{q}$  strongly depend on the parity of  $q$ . And so, it is not a surprise that the study of the general case splits into two sub-cases which are determined by the parity of  $q$ . The case when  $q$  is even is rather easy. Thanks to a trick of [Margenstern 2002] which was found in the study of [Margenstern 2003d], the case when  $q$  is odd is scarcely more complex.

##### 4.1.1 The case when $q$ is even

In this case, we take an angular sector with an angle  $\frac{2\pi}{q}$  as the head  $S_0$  of the basis of splitting. Below, figure 6 illustrates the splitting of  $S_0$ . Along  $p-3$  sides of the leading polygon  $\Pi$  of  $S_0$  and outside it, we can delimit  $h-1$  copies of  $S_0$ : indeed, the angle which is left outside  $\Pi$  and which is delimited by the continuation of the other side has a value of  $(h-1) \cdot \frac{2\pi}{q}$ , where  $h = \lfloor \frac{q}{2} \rfloor$ .

When proceeding in this way from the left to the right, we see that when we arrive at the other side of the angular sector  $S_0$ , we find a region  $S_1$  which we call a **truncated angular sector**, see [Margenstern 2002, Margenstern 2003a].

Therefore, the region  $S_0$  splits into one leading pentagon  $\Pi$ ,  $(p-3) \cdot (h-1)$  regions  $S_0$  and one region  $S_1$ . We represent this by:

$$(a) \quad S_0 \longrightarrow (p-3) \cdot (h-1) \cdot S_0 + S_1$$

And now, we have to split the truncated angular sector  $S_1$  which we have just found. The region is characterized by the complement of the vertex angles to  $\pi$ : it is  $\frac{2\pi}{q}$  in both cases.

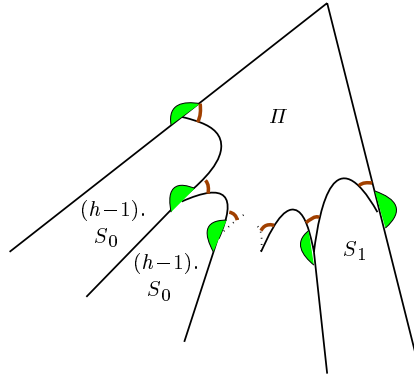


**Figure 6** The splitting of  $S_0$ , when  $q$  is even.

The splitting of  $S_1$  is given by figure 7, below.

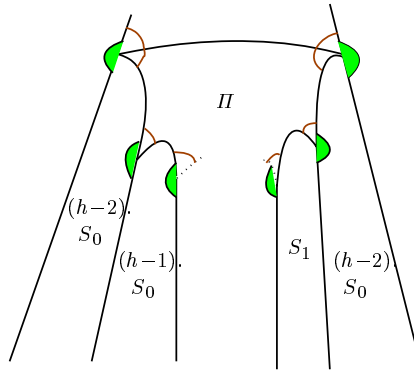


**Figure 7** The splitting of  $S_1$ , when  $q$  is even.

Now, the region  $S_1$  splits into one leading pentagon  $II$ ,  $(p-2).(h-1)-2$  regions  $S_0$  and one region  $S_1$ . Thus, we write this:

$$(b) \quad S_1 \longrightarrow ((p-2).(h-1)-2).S_0 + S_1$$

It is important to note that the splitting of  $S_1$  involves the same regions  $S_0$  and  $S_1$ .

#### 4.1.2 The case when $q$ is odd

The case when  $q$  is odd seems at first more difficult: if we take the same angular sector as previously to play the rôle of  $S_0$ , we cannot divide the complement of

the angle vertex into an integral number of copies of the angular sector. The difficulty can be turned out by introducing right-hand and left-hand parts of  $S_0$  in order to take into account the half term which appears when we divide  $q$  by 2.

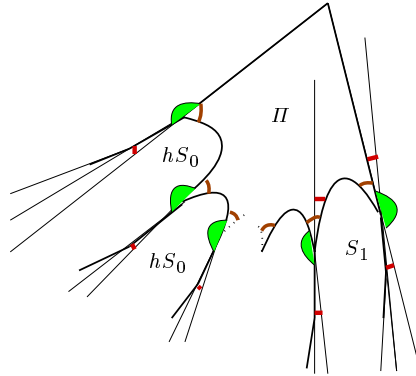


**Figure 8** *The splitting of  $S_0$ , when  $q$  is odd.*

Fortunately, there is a simpler solution. Using a way which is indicated in [Margenstern 2003a], we distort the previous regions in order to overcome the problem of the half: we withdraw such a half on one side, and we give it back to the region on the other side. The process is recursively repeated at each vertex of the leading tiles. On each side, this allows us to have integral multiples of the vertex angle. And so, we define the new line to be on the left-hand side of the bisector of the vertex angle. The region which is defined in this way is called a **distorted** angular sector  $S_0$ . Analogously, we define the region  $S_1$  as indicated in figures 8 and 9.

We obtain that the region  $S_0$  splits in a very similar way to the case when  $q$  is even. Here we have:

$$(c) \quad S_0 \longrightarrow (p-3).h.S_0 + S_1$$

This time, region the  $S_1$  splits a bit differently as in the case when  $q$  is even. For the new splitting of  $S_1$  we can write:

$$(d) \quad S_1 \longrightarrow ((p-2).h-3).S_0 + S_1$$

It should be noted that in the odd case, this construction cannot be performed when  $q = 3$ : the definition of the deviation which is introduced with respect to the bisector of the vertex angle would lead us to a side of the same polygon. But in [Margenstern et al. 2004a, Margenstern et al. 2004b], this situation is dealt with enough details.

Here, we again remark that  $S_1$  can be split in terms of  $II$ ,  $S_0$  and  $S_1$  only: no additional region is involved.

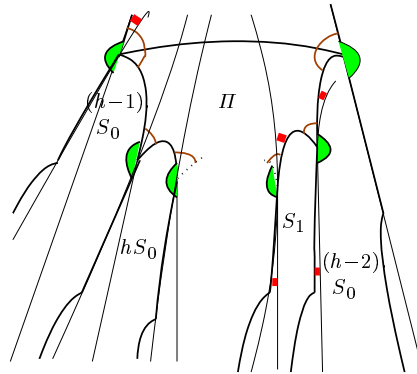


Figure 9 The splitting of  $S_1$ , when  $q$  is odd.

### 4.2 Matrices and polynomials

And so, we can re-write the above relations (a), (b), (c) and (d) using a matrix which will be both an incidence- and a counting matrix as indicated below:

$$M_\epsilon = \begin{vmatrix} (p-3).h_\epsilon & 1 \\ (p-2).h_\epsilon - 2 - \epsilon & 1 \end{vmatrix},$$

where  $h = \lfloor \frac{q}{2} \rfloor$  and  $h_\epsilon = h - 1 + \epsilon$ , with  $\epsilon = q \pmod 2$ . This allows us to give a unique formulation, independent of the parity of  $q$ .

From this, we easily obtain the characteristic polynomial of  $M_\epsilon$  with a unique expression depending on the parity of  $q$ :

$$P_\epsilon(X) = X^2 - ((p-3).h_\epsilon + 1).X - h + 3,$$

It is not difficult to prove that  $P_\epsilon(X)$  has a dominant root  $\beta_\epsilon$  which satisfies the estimation  $b_\epsilon - 1 < \beta_\epsilon < b_\epsilon + 1$ , where we put  $b_\epsilon = (p-3).h_\epsilon + 1$ .

Indeed, as  $P_\epsilon(1) = 1 - b_\epsilon - h + 3$ , we easily obtain that  $P_\epsilon(1) = -(p-2).h_\epsilon + 2 + \epsilon$ . As we assume  $q \geq 5$ , we get that  $h_\epsilon \geq 2$ . As we have  $p \geq 4$ , we get  $(p-2).h_\epsilon \geq 4$ , hence  $P_\epsilon(1) \leq -1$ .

Similarly,  $P_\epsilon(-1) = 1 + b_\epsilon - h + 3$  from which we get the following value  $P_\epsilon(-1) = 4 + \epsilon + (p-4).h_\epsilon \geq 4$ . And so,  $P_\epsilon(-1) > 0$ .

This is enough to conclude that there is a greatest real root  $\beta_\epsilon$  which is a Pisot number. But easy computations give us  $P_\epsilon(b_\epsilon) = -h + 3$ ,  $P_\epsilon(b_\epsilon - 1) = P_\epsilon(1) < 0$  and  $P_\epsilon(b_\epsilon + 1) = P_\epsilon(-1) > 0$ .

#### 4.2.1 The language of the splitting

The proof of theorem 2 about the language of the splitting, when  $p, q \geq 4$  follows from what we established in the previous section and also from theorem 8.1 of [Hollander 1998] in the case when the polynomial has a Pisot number.

And so, we know that the language of the splitting for the tilings  $\{p, q\}$  is regular when  $p \geq 4$ . As in our case the polynomial of the splitting has a Pisot number among its root, there is a general characterization of the language which is given in [Lothaire 2002], chapter 7, proposition 7.3.6.

**Theorem 4** – *Let  $\mathcal{L}$  be the language of the splitting corresponding to tiling  $\{p, q\}$  when  $p \geq 4$ . Then,  $\alpha_k \dots \alpha_0 \in \mathcal{L}$  if and only if  $\alpha_k \dots \alpha_0 \leq_{\mathcal{L}} \mathcal{A}(u_k - 1)$ , where  $\leq$  denotes the lexicographic order over the alphabet of the language, and where  $\mathcal{A}(n)$  is the representation of  $n$  in  $\mathcal{L}$ .*

Although we know that almost all languages of the tilings  $\{p, q\}$  are regular, they are very different. In the classical case of the pentagrid, the consequence of the above condition is that some pattern is ruled out, namely, any occurrence of 11. Here, in the general case, we also have the interdiction of some pattern, but we also have the opposite phenomenon.

This can be illustrated by the following example. Consider the case when  $p = 7$  and  $q = 8$ . The polynomial is  $P(X) = X^2 - 13X - 1$ . Accordingly,  $b = 13$  and let  $b_1 = 12$ . It is not difficult to see that  $u_{2n+1} - 1$  is represented by  $(b0)^n$  and that  $u_{2n} - 1$  is represented by  $(b0)^{n-1}b_1$ . And so, in this case, we can see that  $b$  may appear and, when this is the case, it must be followed by 0. We shall see other such cases in the next section.

## 5 Rules for the tree generation

As announced in the introduction, here we give the tools which are needed for the algorithms which will be displayed in the next section. These tools take the form of **rules** which, applied to a tile, allow us to get the coordinates of its neighbours. The rules also allow us to restore the dual graph of the tiling, starting from the spanning tree of the splitting.

To this purpose, we shall use the property that the polynomial has a Pisot root and, as a consequence, that the language of the splitting is regular. Taking advantage of theorem 3, we shall indicate rules to compute the neighbours of a node. This time, there will be no difference between the cases odd  $q$  and even  $q$ : the characteristic polynomial behave in the same way in both cases. The difference is in the values of the coefficients, not in the properties of the roots.

The polynomial can be rewritten as:

$$P(X) = X^2 - bX - k,$$

with  $b = (p-3)h_\epsilon + 1$  and  $k = h - 3$ .

*A priori*, we have three cases, depending on the sign of  $k$ :  $k$  negative,  $k = 0$  and  $k$  positive. Note that the case when  $k$  is negative contains the case  $h = 2$



only:  $h = 0$  does not have a meaning, whatever the parity of  $q$  is;  $h = 1$  has no meaning when  $q$  is even and when  $q$  is odd, it is a case which was studied in already quoted papers;  $h = 2$  was briefly reminded in section 2 when  $q$  is even. When  $q$  is odd, this corresponds to  $q = 5$ , a case which we shall study a bit further. The case when  $h = 3$  means  $q = 6$ , when  $q$  is even, and  $q = 7$ , when it is odd. In this case, the induction equation reduces to  $u_{n+1} = bu_n$ . We shall start with this case. Later, we have the case when  $h = 4$  which, independently on the parity, is a bit different from the general case  $h > 4$ . We shall see that the preferred son property is true when  $h \leq 4$  and that it is not true when  $h > 4$ .

**5.1 The particular cases**

**5.1.1 The case  $h = 3$**

We know that  $u_{n+1} = bu_n$ . This means that the language of the splitting is the set of all the words on alphabet  $[0..b_1]$ , where  $b_1 = b-1$ , which starts with a digit, different from 0.

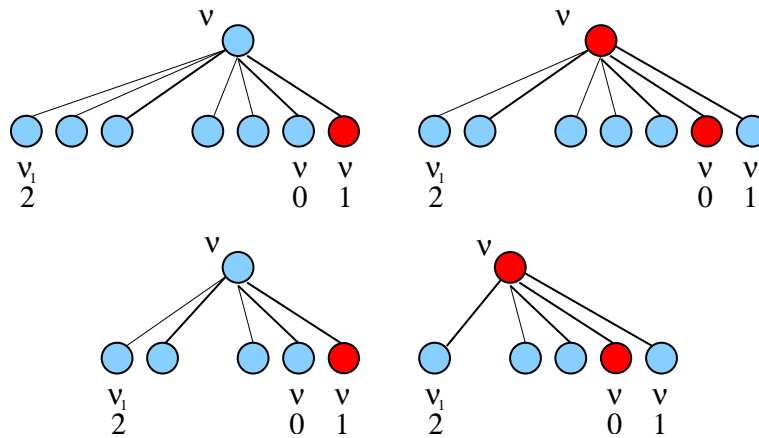


**Figure 10** The rules for the tree when  $h = 3$ .  
 Above,  $q = 7$ ; below, even  $q = 6$ .

Above, figure 10 indicates the rules for finding the coordinates of the sons of a node from its coordinate. Indeed, the rules of figure 10 do not depend on the parity of  $q$ . The nodes have always  $b$  sons. If the node  $\nu$  is white, its last son is black and all others are white. If the node is black, the black son is the penultimate. The coordinates of the sons are:  $\nu_1 2$  for the first,  $\nu_1 i$  for the  $i-1^{\text{th}}$ ,  $\nu_0$  for the penultimate and  $\nu_1$  for the last, where  $\nu_1$  is the writing of  $\nu-1$ , again taking the maximal representation. It is plain that the rule is true for the root of the tree and the node 2. Then it is easily proved by induction on the nodes,

as the number of the nodes is  $b$  whatever the node is white or black. From the rules, it is clear that the preferred son property also holds in this case, whatever the parity of  $q$  is.

Next, figure 11 illustrates the splitting of the basic regions in these cases.

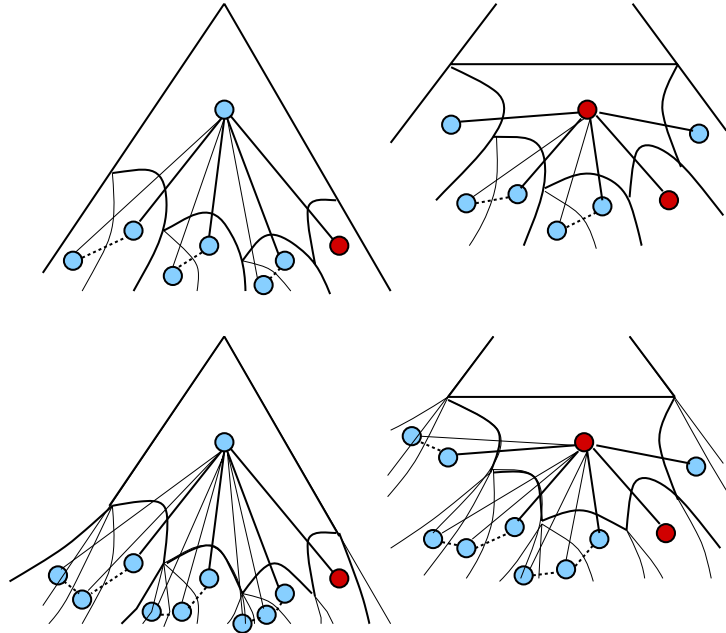


**Figure 11** *The splitting when  $h = 3$ .  
Above, even  $q = 6$ ; below, odd  $q = 7$ .*

### 5.1.2 The case $h = 2$ , odd $q$

We turn now to the case when  $q = 5$  which corresponds to  $h = 2$  and odd  $q$ . In this case, it is useful to have a look at the writing of  $u_n - 1$ , as suggested by theorem 3. As, by definition, we take  $u_0 = 1$ , it is the root, a simple computation gives us  $u_1 - 1 = b_1$ , again using  $b_1$  to denote  $b - 1$ . Next,  $u_2 = bu_1 - u_0$  and so,  $u_2 - 1 = b_1u_1 + u_1 - u_0 - 1 = b_1u_1 + b_2$ , where  $b_2 = b - 2$ . As an induction hypothesis, assume that  $u_n - 1 = b_1u_{n-1} + b_2 \sum_{i=0}^{n-2} u_i$ . Then, applying the induction hypothesis and the induction equation of  $u_n$ , we obtain the following computation:

$$u_{n+1} - 1 = bu_n - u_{n-1} - 1 = b_1u_n + u_n - 1 - u_{n-1} = b_1u_n + b_2 \sum_{i=0}^{n-1} u_i.$$

And so, the induction hypothesis is proved.

We shall summarise this result by writing  $u_n - 1 \simeq b_1 b_2^{n-1}$ .

For this case, we have the rules which are illustrated by figure 12, below. A bit further, figure 13 illustrates the splitting. Note that in this case, the white nodes have  $b$  sons while the black ones have  $b_1 = b - 1$  of them.

It is not difficult to prove the following property, by induction:

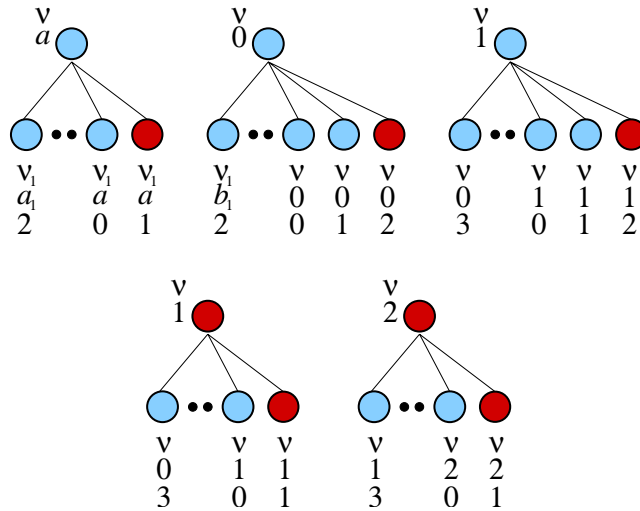


**Figure 12** The rules when  $h = 2$ , with odd  $q$ . Above, the rules for the white nodes, where  $a \notin \{0, 1\}$  and  $a = a_1 + 1$ . Below, the rules for the black nodes.

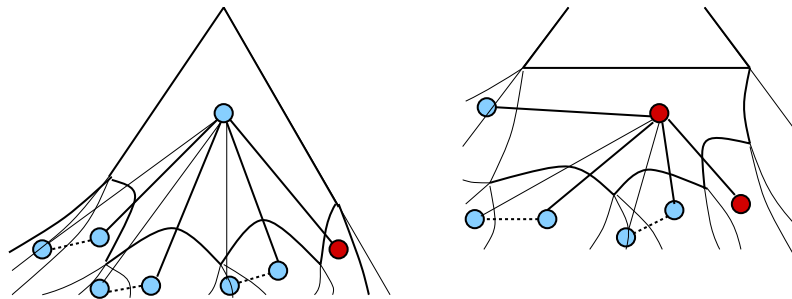


**Figure 13** The splitting when  $h = 2$ , with odd  $q$ . On the left-hand side,  $S_0$ , on the right-hand side:  $S_1$ .

**Lemma 1** – When  $q = 5$ , which entails  $h = 2$ , the black nodes end in 1 or 2. The preferred son property holds. The black son of a node is always the last one. The continuator is the penultimate son for the black nodes and the white nodes which do not end in 0 or 1. For the white nodes in 0 and 1, the continuator is the son which is before the penultimate. Note that a black node in 1 follows a

white node which ends with a single 0. A black node in 2 follows a white node in 01 or in 11.

Proof. From the rules, a white node  $\nu$  with a single ending 0 occurs in a rule of a white node which does not end in 0 or in a black node. Then, the node which follows  $\nu$  is a black node in 1. From the rules, we can see that it is followed by a white node in 2, hence with a standard white rule, *i.e.* which is applied to the nodes which do not end in 0 or 1. From the rules, a white node with at least two ending 0's is followed by a white node in 1 and then a black node in 2. From the rules we can see that the next white node, in 3, fits with the application of the expected standard rule. ■

### 5.1.3 The case $h = 4$

Before turning to this case, we explain why we distinguish this case from the general case  $h > 4$ .

First, as now  $k \geq 1$ , we remark that  $P(b) = -k$  and so,  $b < \beta$ , where  $\beta$  is the greatest real root of the polynomial of the splitting. Accordingly, the coordinates of a node make use of the alphabet  $\{0..b\}$ . However, there is a difference between the case  $k = 1$ , or  $h = 4$ , and the general case, when  $k > 1$ , or  $h > 4$ . The reason is the following lemma about the writing of  $u_n-1$ :

**Lemma 2** – *The sequence  $\{u_n\}_{n \in \mathbb{N}}$  of the numbers of nodes on the levels of the spanning tree of the splitting for a tiling  $\{p, q\}$  satisfies the following property:*

$$u_{2n}-1 \simeq (bk_1)^n \quad \text{and} \quad u_{2n+1}-1 \simeq (bk_1)^n b_1,$$

where  $k_1 = k-1$ .

**Corollary 1** – *Let  $U_n$  be defined by the following induction equations:*

$$U_0 = u_0;$$

$$U_{n+1} = U_n + u_{n+1}.$$

$$\text{Then: } u_{n+1} = U_n + \sum_{i=1}^{\lfloor \frac{n+1}{2} \rfloor} ((b-1)u_{n+2-2i} + (k-2)u_{n+1-2i})$$

with the convention that  $u_{-1} = u_{-2} = 0$ .

Proof of lemma 2. The proof is by induction and it is clearly true for  $u_1$  and  $u_2 = bu_1 + ku_0$ , from which we get  $u_2-1 = bu_1 + (k-1)u_0 \simeq bk_1$ . Assume that the lemma is true for  $u_{2n}-1$  and for  $u_{2n+1}-1$ . Now:

$$u_{2n+2}-1 = bu_{2n+1} + ku_{2n}-1 = bu_{2n+1} + (k-1)u_{2n} + u_{2n} - 1$$

$$\simeq b0^{2n+1} + k_1 0^{2n} + (bk_1)^n \simeq bk_1 0^{2n} + (bk_1)^n = (bk_1)^{n+1}.$$

Replacing,  $u_{2n+2}$ ,  $u_{2n+1}$  and  $u_{2n}$  by, respectively,  $u_{2n+3}$ ,  $u_{2n+2}$  and  $u_{2n+1}$ , we get the proof of the relation for  $u_{2n+1}$ . ■

Proof of corollary 1. It is easy to rewrite the computations of lemma 2 into a single formula as follows:

$$u_n = 1 + \sum_{i=1}^{\lfloor \frac{n}{2} \rfloor} (bu_{n-2i+1} + (k-1)u_{n-2i}) + b_1u_{n-2\lfloor \frac{n}{2} \rfloor - 1}.$$

As  $u_0 = 1$ , taking  $u_i$  from each term of the sum, we get the result. ■

And so, when  $h > 4$ ,  $k - 2 \geq 0$ , and so, each term of the sum indicated in corollary 5 is non-negative. Accordingly, the sum is positive, which proves that  $U_n + b_1u_n < u_{n+1} < U_{n+1}$ . The second inequality is obvious from the definition of  $U_n$ , and the first one is a direct consequence of corollary 1. Now, when  $h = 4$ ,  $k - 2 < 0$ , and so, the relation  $U_n + b_1u_n < u_{n+1}$  is no more true.

	1	...	$b-2$	$b-1$	$b \bullet$
$\nu a$	$\nu a_1 2$	...	$\nu a_1 b_1$	$\nu a 0$	$\nu a 1$
$b_1 B \nu 0$	$\nu_1 b_1 3$	...	$\nu_1 b 0$	$\nu 0 0$	$\nu 0 1$
$b 0 B \nu 0 0$	$\nu_1 b 0 2$	...	$\nu_1 b 0 b_1$	$\nu 0 0 0$	$\nu 0 0 1$
$b_1 W \nu 0$	$\nu_1 b_1 2$	...	$\nu_1 b_1 b_1$	$\nu_1 b 0$	$\nu 0 0$
$b 0 W \nu 0 0$	$\nu_1 b 0 1$	...	$\nu_1 b_1 b_2$	$\nu_1 b_1 b_1$	$\nu 0 0 0$

	1	...	$b-1 \bullet$	$b$	$b+1$
$b_1 \nu 0 0$	$\nu_1 0 b_1 2$	...	$\nu_1 0 b 0$	$\nu 0 0 0$	$\nu 0 0 1$
$b 0 \nu 0 0$	$\nu_1 b 0 1$	...	$\nu_1 b 0 b_1$	$\nu 0 0 0$	$\nu 0 0 1$
$\nu b_1 0$	$\nu b_2 b_1 2$	...	$\nu b_2 b 0$	$\nu b_1 0 0$	$\nu b_1 0 1$
$\nu b 0$	$\nu b_1 b_1 2$	...	$\nu b_1 b 0$	$\nu b 0 0$	$\nu b 0 1$
$\nu 1$	$\nu 0 1$	...	$\nu 0 b_1$	$\nu 1 0$	$\nu 1 1$
$\nu b_1$	$\nu b_2 2$	...	$\nu b_1 0$	$\nu b_1 1$	$\nu b_1 2$

**Table 1** Rules for the case  $h = 4$ :  
 first table: white nodes;  $a \neq 0$ ,  $a = a_1 + 1$ ;  
 second table: black nodes;  $b_1 = b_2 + 1$ .

Now, the inequality  $U_n + b_1u_n < u_{n+1}$  means that the change from  $\ell$  digits to  $\ell+1$  happens in the sub-tree of the spanning tree which is rooted in the last son of

the root which is a black node. In the cases  $h = 2$  and  $h = 3$ , we can see that the change to an additional digit happens in the penultimate sub-tree, recursively for the case  $h = 3$ . For the case  $h = 2$ , this change happens in the penultimate tree for the first time and later, it always happens in the ante penultimate one, recursively. When  $h = 4$ , we shall see that the change always happen in the penultimate sub-tree, recursively. In case  $h > 4$ , we shall see that it happens in the penultimate sub-tree of the root and later, it happens in the  $b^{\text{th}}$  sub-tree, thanks to the relation  $U_n + b_1 u_n < u_{n+1}$ .

Starting from this case, we display the rules in a table instead of a figure. Above, the first row of the table indicates a number for the sons of the node: this number is relative to the node. It runs from 1 up to  $b$  for the white nodes, which is the case of the first table. It runs from 1 up to  $b+1$  for the black nodes. In both cases, the black son is signaled by a bullet: it falls on the last node for the white nodes, on the node with rank  $b-1$ , the ante penultimate, for the black nodes. Next, on each row, under each number, we schematically indicate the writing of the coordinate of the corresponding son. In fact we indicate the writing for the first node and for the two or three last ones as for the others, it is obvious from the first one.

Now it can be understood that the relevant information is displayed in the table in the same way as it is in the figures and in the same order. And so, all what is significant is present. There is an advantage to this compact form: it more efficiently allows us to check the properties indicated by the table itself, by induction on the levels and, on each level, on the rank of the node.

Let us look at this point more precisely. With respect to the previous cases, here, there is also another difference. As  $k > 0$ , black nodes have more sons than white ones. In the case  $h = 4$ , white nodes have  $b$  sons and black nodes have  $b+1$  of them. From the splitting, which is illustrated by the general figures 8 and 9, we check that in white nodes the black son is the last and that in black nodes it is the ante penultimate as just indicated above.

Now, in order to proceed to the above indicated induction, the rows of the table indicate two additional informations on the father of the node whose coordinates are indicated in the entries of the row in the table. We indicate in a column which precedes the first one the information which concerns the father of the node whose sons are displayed by the table. In the first table, the information for the father is the writing of its coordinate, its status, *i.e.* white or black, and the last or last two digits of the node which precedes the father on its level. In the second table, as the father is a black node, it is not needed to indicate the status of its preceding nodes on its level as it is always white. However, in a few cases, it is useful to know the last digit of the preceding node, when there can be an ambiguity. This is why we have two cases for the nodes ending in 00. Note that in the first table,  $\nu 0$  means that the number of ending 0's is odd and  $\nu 00$

that this number is even.

Note that the first line of the first table applies for the root whose coordinate is 1. For the level 1, we start from the leftmost node whose coordinate is 2: again, the first row of the first table apply. It is easy to show, by induction, that the leftmost son of the level  $n$  has the coordinate  $1^{n-1}2$  and that the rightmost son of the same level has the coordinate  $1^{n+1}$ . Now, from the leftmost son on the level 1 which is written 2 and whose leftmost son is 12, we can easily check that the first row of the first table applies to the node 2. The same row applies until the node  $b_1$ , which give, for the sons:  $b_22 \dots b_2b_1 b_10 b_11$ . Next, come the node 10 for which we have the following sons:  $b_12 \dots b_1b_1 b0 100$ , which corresponds to the row 4 of the first table. Then we have the last node of the level 1 which is 11 and whose son are:  $101 \dots 10b_1 110 111$  which corresponds to the row 5 of the second table. We check again the induction hypothesis on the leftmost and rightmost nodes of a level and for the leftmost node on the next level, we clearly have to apply again the row 1 of the first table.

Now, we can see that, in the row 1, the black son ends in 1, that in the row 4, it ends in 00 and that in the row 5 of the second table, it ends in  $0b_1$ . This indicates new lines in the second table which, in their turn give rise to new endings in both tables. The induction process shows that this increasing of the tables quickly converges to the tables which are displayed by table 1.

This induction process is a double induction on the level and the rank of a node in its level that these rules allow to construct the spanning tree. Note that the coordinate of the previous node is easy to compute thanks to lemma 4. In this case, also note that the alphabet is  $\{0..b\}$  and that  $b$  occurs except as a last digit which is always different from  $b$ . When  $b$  occurs, it is immediately followed by 0 and only this digit.

However, the status of a node, white or black, is not easily inferred from the numbering. We shall give more precision, later, in the case  $h > 4$ . The simplest solution is to consider that the status is a part of the coordinate. In order to avoid a rather complex computation, the simplest way is to store the full coordinate of a node and both its status and the status of its previous neighbour on the same level. The rules allow to compute for each son its coordinates and its status together with the same information for the previous son or neighbour of the same level. Using the tables and the same induction, we can prove that two consecutive white nodes in 0 are followed by a black node which, of course, is in 1.

The rules show that the preferred son property is true also in this case. However, we can see a phenomenon which will be amplified in the general case and which will alter the preferred son property. When a node in 0 follows a node in  $b_1$ , the rules show that the node in 0 has two sons ending in 0 which are consecutive. If the node has coordinate  $\nu 0$ , these sons have coordinates  $\nu_1 b0$

and  $\nu 00$ . This comes from the fact that  $b1$  is rewritten  $100$  in the maximal representation as  $bu_{n+1} + u_n = u_{n+2}$  is the basic induction equation. We remark that  $\nu_1 b \simeq \nu 0$  but  $\nu_1 b 0 \neq \nu 00$  which can easily be checked.

### 5.2 The general case

Now, we turn to the case when  $h > 4$ .

As already indicated with the case  $h = 4$ , this case has the property that  $U_n + b_1 u_n < u_{n+1}$ . This means that the change in the number of digits which occurs at each level happens in the last sub-tree of the spanning tree. The intuitive reason is that before going to  $10$ , we have to mark  $b0$ ,  $b1$  and so on until we arrive at  $bk_1$ . And we have to write  $100$  just after  $bk_1$  in the maximal representation. Again, note that  $bk \simeq 100$ . Another difference with the previous cases is that the white nodes still have  $b$  sons while the black ones have much more of them:  $b+k$ . This explains the alteration for the preferred son property: take a white node  $\nu b 0$  and assume that its first son is  $\nu_1 b_1 b_1 2$ , as indicated in tables 2 below, where  $\nu = \nu_1 + 1$ . Then, the single son ending in  $0$  is  $\nu_1 b_1 b 0$  and it is the penultimate. If the preferred son property were true, we would find  $\nu b 00$  and it is plain that  $\nu b 00 \not\simeq \nu_1 b_1 b 0$ . However, as  $\nu_1 b_1 b \simeq \nu b 0$ , we can say that the node  $\nu_1 b_1 b 0$  contains the number of its father as a shortened representation of this number. But there is a worse situation which is indicated in the table for a sub-class of white nodes ending in  $1$ . For such a node  $\nu a 1$ , the first node is  $\nu a_1 b 2$  and the single node in  $0$  is  $\nu a 00$  which has rank  $k-1$  among the sons of the node. This is not the preferred son property which would require  $\nu a 10$  somewhere among the sons and also  $\nu a 00$  does not contain the number of the father. Here, there is a delay in the numbering of the sons with respect to the fathers. We shall explain this a bit further. We can see from the table that besides these two cases, for all other nodes, the preferred son property is true.

Also in the general case, the notion of **status** of a node is a bit more complex. We define nodes with  $b$  sons as white and nodes with  $b+k$  sons as black, as previously. However, we append an additional information concerning the coordinate of the first son of the node and its last one. It is not difficult to check that for most white nodes  $\nu a$ ,  $a \neq 0$ , belonging to the levels  $1, 2$  and  $3$ , the first node is  $\nu a_1 2$  where  $a = a_1 + 1$ , and the last one is  $\nu a 1$ . But there are other possibilities: for instance, the first son can be  $\nu a_1 k''$  where  $k' = k + 1$  and  $k'' = k + 2$ , and the last one is then most often  $\nu a k'$ . A third class of white nodes have the following pattern: the node is still  $\nu a$ , the first son is  $\nu a_1 \alpha''$  and the last one is  $\nu a \alpha'$ . We shall use letters **o**, **1** and **2** to denote these patterns as follows:

denotation	first node	last node
<b>o</b>	$2$	$1$
<b>1</b>	$k''$	$k'$
<b>2</b>	$\alpha''$	$\alpha'$



As we shall see, for a few nodes, the patterns can be mixed: the first son can follow one pattern and the last one can follow another. This is why in the table we write node  $\nu$  as  $\mathbf{u} \nu \mathbf{v}$ , where  $\mathbf{u}$  denotes the pattern followed by the first son and  $\mathbf{v}$  denotes the pattern followed by the last son.

Now we can precisely define the **status** of a node: it is the indication of its colour and of the patterns followed by its first and last sons. It can be denoted as  $\mathbf{u}C\mathbf{v}$ , where  $C \in \{B, W\}$  is the colour of the node,  $\mathbf{u}$  is the pattern followed by the first son and  $\mathbf{v}$  is the pattern followed by the last one.

	1	...	$b-1$	$b$	•
$\circ \nu a \circ$	$\circ \mu d_1 2 \circ$	...	$\circ \nu a 0 \circ$	$\circ \nu 0 1 \circ$	
$\circ \nu 0 \circ$	$\circ \nu_1 b_1 2 \circ$	...	$\circ \nu_1 b 0 \circ$	$\circ \nu_1 b 1 \circ$	
$\circ \nu 0 0 \circ$	$\circ \nu_1 b k_1 2 \circ$	...	$\circ \nu 0 0 0 \circ$	$\circ \nu 0 0 1 \circ$	

	1	...	$\alpha-1$	$\alpha$	...	$b-1$	$b$	•
$1 \nu a 1$	$\circ \nu a_1 k'' \circ$	...	$\circ \nu a 0 \circ$	$\circ \nu a 1 2$	...	$2 \nu a k 2$	$2 \nu a k' \circ$	
$1 \nu 0 \circ$	$\circ \nu_1 b_1 k'' \circ$	...	$\circ \nu_1 b 0 \circ$	$\circ \nu_1 b 1 2$	...	$2 \nu 0 0 2$	$2 \nu 0 1 \circ$	

	1	...	$k-1$	$k$	...	$b-1$	$b$	•
$2 \nu a 2$	$1 \nu a_2 \alpha'' 1$	...	$1 \nu a_1 0 \circ$	$\circ \nu a_1 1 \circ$	...	$\circ \nu a_1 \alpha \circ$	$\circ \nu a_1 \alpha' 1$	
$2 \nu 0 0 2$	$1 \nu_1 b k_1 \alpha'' 1$	...	$1 \nu 0 0 0 \circ$	$\circ \nu 0 0 1 \circ$	...	$\circ \nu 0 0 \alpha \circ$	$\circ \nu 0 0 \alpha' 1$	
$\circ \nu a 1 2$	$\circ \nu a_1 b 2 \circ$	...	$\circ \nu a 0 0 \circ$	$\circ \nu a 0 1 \circ$	...	$\circ \nu a 0 \alpha \circ$	$\circ \nu a 0 \alpha' 1$	

	1	...	$k-1$	...	$b-1$	•	...	$b+k-1$	$b+k$
$\circ \nu 1 \circ$	$\circ \nu_1 b 2 \circ$	...	$\circ \nu 0 0 \circ$	...	$\circ \nu 0 \alpha 1$	...	$1 \nu 1 0 \circ$	$\circ \nu 1 1 \circ$	
$2 \nu 0 1 \circ$	$1 \nu_1 b k_1 \alpha'' 1$	...	$1 \nu 0 0 0 \circ$	...	$\circ \nu 0 0 \alpha 1$	...	$1 \nu 0 1 0 \circ$	$\circ \nu 0 1 1 \circ$	
$\circ \nu 0 \alpha 1$	$\circ \nu 0 \alpha_1 2 \circ$	...	$\circ \nu 0 \alpha_1 k \circ$	...	$\circ \nu 0 \alpha 0 \circ$	...	$\circ \nu 0 \alpha k \circ$	$\circ \nu 0 \alpha k' \circ$	
$2 \nu k' \circ$	$1 \nu k_1 \alpha'' 1$	...	$1 \nu k 0 \circ$	...	$\circ \nu k \alpha 1$	...	$1 \nu k' 0 \circ$	$\circ \nu k' 1 \circ$	
$\circ \nu \alpha' 1$	$\circ \nu \alpha 2 \circ$	...	$\circ \nu \alpha k \circ$	...	$\circ \nu \alpha' 0 \circ$	...	$\circ \nu \alpha' k \circ$	$\circ \nu \alpha' k' \circ$	
$\circ \nu c 0 \circ$	$\circ \nu c_1 b_1 2 \circ$	...	$\circ \nu c_1 b_1 k \circ$	...	$\circ \nu c_1 b 0 \circ$	...	$\circ \nu c 0 0 \circ$	$\circ \nu c 0 1 \circ$	

**Table 2** Rules for case  $h > 4$ :

first table: the ordinary white nodes, with pattern  $\circ$  for the first and the last sons; note that  $a \neq 0$ ; when  $a_1 = 0$ ,  $\nu 0 \simeq \mu d$ ,  $d \in \{b, k\}$ ; when  $a_1 \neq 0$ ,  $\mu = \nu$  and  $d_1 = a_1$ ;  
 second table: the white nodes in pattern **1** for the first and last sons; also white nodes  $\nu$  with  $1 \nu \circ$ ;

*third table: the white nodes in pattern 2 for the first and last sons; also white nodes  $\nu$  with  $\circ \nu 2$ ; here,  $a_2 = a-2$ ;*  
*fourth table: the black nodes; in the last row,  $c$  stands for  $\alpha$ ,  $\alpha'$  or  $b$ .*

In these tables, we also use the following convention: we write  $x_1$  for  $x-1$ . This is due to the fact that we consider  $x_1$  as a digit. We also defined  $\alpha = b-k$ , again a digit.

For most white nodes, as the number of nodes is  $b$  and as adding  $b$  changes the penultimate digit to its successor, this is the reason why the first and last sons follow the same pattern, most often. There are two reasons for the change of one pattern to another. The first reason is that the change of the last digit into 0 may occur much sooner: at rank  $k-1$  for a node with a first node in pattern  $\circ$ . Usually, this will then entail pattern 2 for the last son. Another reason is the presence of a black node. As it has  $b+k$  nodes, this breaks the  $b$ -periodicity of the white nodes.

However, black nodes are rare in comparison with white ones and most often, they occur at the right place: with a first node following pattern  $\circ$ , when rank  $b-1$  is reached, we turn to 0 as under a standard white node. But, this time, the penultimate digit turns from  $b_1$  to  $b$ . Accordingly,  $k$  nodes further, we have  $bk$  as the last two digits and so, this turns to 00 with a carry, possibly propagating to other digits. Consequently, the last node is in 01, again pattern  $\circ$ . However, this is not always the case, and tables 2 indicate all the possibilities.

Note that for the white nodes in 0, the indication of the table are in agreement with the parity of the number of ending 0's: 00 indicates an even positive number of 0's; a single 0 indicates an odd number of them.

Now, it is a tedious but not difficult exercise to check that the rules of the table allow to construct the tree, by induction on the levels and, for each level, on the rank of the nodes in the level. The beginning of the argument is exactly the same as what we did in the case  $h = 4$ . We can observe that all configurations of nodes which appear in the table also appear as first entry of a line. We can also check that the patterns match: the pattern of the last son of a node is the pattern of the first son of the next node on the same level or, if we are at the last node on the level, with the first node on the next level.

Note that if we know the coordinates and the status of a node and the status of its predecessor on the level, we can compute the coordinates and the status of the next node on this level.

As a final remark, let us consider the number of rules which are used for the generation of the spanning tree according to the method which is indicated here. In the case  $h = 3$ , there are four rules, independently of  $p$ . In the case  $h = 2$  with odd  $q$ , the number of rules depends on  $b$ . Note that in figure 12, the rules for the nodes  $\nu a$  with  $a \notin \{0, 1\}$  are represented by a single picture which we

define as a **scheme rule**. Note that we could replace this scheme rule by the following one:

	1	...	$b-1$	$b$	•
$\nu$	$\nu_1 2$	...	$\nu 0$	$\nu 1$	

where  $\nu = \nu_1 + 1$ . This new rule is used with the others according to the following priority principle: first apply rule  $\nu 1$  if the node matches this form; if not, apply  $\nu 0$  with the same condition; if none of the previous rules matches the form of the node, apply the above rule. Call **mutification** the above transformation of the rule for the nodes  $\nu a$ ,  $a \notin \{0, 1\}$  and **priority scheme** the use of priority with mutification of rules.

Similar remarks can be formulated for the cases  $h = 4$  and  $h > 4$ . In the previous case, the number of rules depends on  $p$  and it depends on  $b$  in the second case, *i.e.* it is bounded by  $p.q$ . The number can be made independent of  $p$  and  $q$  by mutification of the three rules for nodes  ${}_0\nu a {}_0$ , nodes  ${}_1\nu a {}_0$  and  ${}_2\nu a {}_2$  and the corresponding priority scheme.

Accordingly, we proved the following result:

**Theorem 5** *The spanning tree of the splitting of the tiling  $\{p, q\}$  can be generated by a finite number of rules. The number of rules is linear in  $p.q$  but it can be made independent of  $p$  and  $q$  by three scheme rules at most or by mutification of the three corresponding rules and the appropriate priority scheme.*

### 6 Neighbours and dual graph: the algorithms

With the previous algorithms, it is now possible to consider the computation of the neighbours of a node starting from the coordinate of the node.

In [Margenstern 2003b], it is proved that there is an algorithm to compute the path from a node to the root of the spanning tree for the splitting of the pentagrid which is linear in time and space in the coordinate of the node. I have an extension of this proof to  $\{p, 4\}$  which was not yet published and which makes use of a different idea. This idea is followed by the present algorithm, the implementation details being here a bit more complex due to the generality of the problem. The idea consists in constructing three paths and the corresponding lists of statuses of the nodes belonging to the paths. The last item in the list is the status of the node and the penultimate is the status of the father of the node. This information is enough to compute the coordinate of the father from the coordinate of the node.

Let us examine tables 2 again. The number of possible statuses for a node is eight:

$${}_0W_0, {}_1W_1, {}_2W_2, {}_1W_0, {}_0W_2, {}_0B_0, {}_2B_0, {}_0B_1.$$

We call **characteristic** of node  $\nu$  the last digit of its coordinate and we denote it by  $\chi(\nu)$ . Call **characteristic configuration** of  $\nu$  the sequence of the characteristics of its sons, from the first one to the last one. For all statuses, except the status  ${}_0B_0$ , there is a single characteristic configuration. For the status  ${}_0B_0$ , there are two characteristic configurations which depend on the characteristic of  $\nu$ . All characteristic configurations are given by table 3, below. In the table, the characteristic of  $\nu$  is indicated only when it is relevant. For each configuration, it can be checked that the number of characteristics is the number of sons of the node.

From this table, it is possible to find out the place of a node which belongs to the path going from the root to  $\nu$ . This depends on the status, and the characteristic of the node. The table indicates that the range of characteristics of a given configuration consists of two or three intervals of remainders modulo  $b$ . Accordingly, these intervals do overlap in the case of a black node. In the case of a white node, they may not overlap. When the intervals do not overlap, the range of the characteristics is the set of all possible remainders. And so, the definition of the next element to append to the path as well as the new digits is easy to determine and needs only a constant amount of information. Note that this situation is the case for the statuses  ${}_0W_0, {}_1W_1$  and  ${}_2W_2$ . For all the other statuses, we have a situation of overlap between the intervals of characteristics.

When an overlap occurs in a configuration, this is caused by a change in the previous digit of the coordinate which turns from one value to the next one. This necessarily happens in the black nodes which have  $b+k$  sons. This also happens in white nodes which have different patterns for the first son and for the last one, namely  ${}_1W_0$  and  ${}_0W_2$ . From table 2, we know that for most nodes, the penultimate digit of the coordinate of the first node of a node  $\nu$ , say  $p(\nu)$ , is the predecessor of  $\chi(\nu)$ . There are a few exceptions: the nodes in 0 and the nodes with the status  ${}_2W_2$ . For the nodes in 0, in fact  $p(\nu) = \chi(\nu-1)$ . For the nodes with status  ${}_2W_2$ , we have  $p(\nu) = \chi(\nu)-2$  when the current digit  $\delta$  satisfies  $1 \leq \delta < k''$ .

status	$\chi(\nu)$	configuration
$\circ W \circ$	-	$2 \dots b_1 0 1$
${}_1 W {}_1$	-	$k'' \dots b_1 0 \dots k'$
${}_2 W {}_2$	-	$\alpha'' \dots b_1 0 \dots \alpha$
${}_1 W \circ$	-	$k'' \dots b_1 0 \dots k_1 0 1$
$\circ W {}_2$	-	$2 \dots k_1 0 \dots \alpha'$
$\circ B \circ$	1	$2 \dots k_1 0 \dots b_1 0 1$
$\circ B \circ$	0	$2 \dots b_1 0 \dots k_1 0 1$
${}_2 B \circ$	-	$\alpha'' \dots b_1 0 \dots b_1 0 1$
$\circ B {}_1$	-	$2 \dots b_1 0 \dots k'$

**Table 3** *Characteristic configurations.*

The promised algorithm is given below, in figure 14.

The body of the loop makes use of a complex procedure which indicates three new nodes. Most often, the third node is useless, but it becomes useful when the previous node had status  ${}_1 W {}_1$  or  ${}_1 W \circ$  and when one of the nodes to be selected has status  ${}_2 W {}_2$ . The three nodes are consecutive nodes on the level and the procedure indicates in  $c$ , where  $c \in \{0..b+k-1\}$ , how to find the first node among the sons of its father. The father is one of the previously computed nodes and it is indicated by  $f_i$ ,  $i \in \{0, 1, 2\}$  as the index of the path whose last node is the expected one.

We have now to explain how the procedure *select* is working in order to check that the algorithm is linear in time and space. The procedure works as follows. The last three digits which were obtained by reading the word  $w$  are stored in the internal variables  $\alpha_2$ ,  $\alpha_1$  and  $\alpha_0$ . These digits are compared with the last three ones of the first and of the last sons of the node indicated by  $\pi_0$ , then by  $\pi_1$  and, at last, by  $\pi_2$ . Table 2 allows us to compute these last digits, using the last three digits of  $w_0$ ,  $w_1$ ,  $w_2$ . At this point we use the following trick: when a carry occurs by decrementing a number, the right writing is present in  $w_0$  or in  $w_1$  if  $w_2$  is used, and so we have simply to switch to the appropriate  $w_i$  and only rewrite its last three digits. From this computations we know the arc to add to which path. Indeed, the number of the arc, in  $\{0..b-1\}$  for the white nodes, in  $\{0..b+k-1\}$  for the black nodes, is appended to the path  $\pi_j$  for the right value of  $j$ . The affiliation of the selected new nodes to the last one of the paths to which they are appended is also fixed at this step of the computation. All of this is performed in constant time.

```

input : w the digits of  $\nu$  ;
d := pop(w) ;
case d is
  when 1       $\Rightarrow \pi_0 := \emptyset ; \pi_1 := 0 ;$ 
                 $w_0 := 1 ; w_1 := 2 ; st_0 := \circ W_{\mathbf{0}} ; st_1 := \circ W_{\mathbf{0}} ;$ 
  when 2 | ... | b1  $\Rightarrow \pi_0 := d-2 ; \pi_1 := d-1 ;$ 
                 $w_0 := d ; w_1 := \mathcal{A}(d+1) ;$ 
                 $st_0 := \circ W_{\mathbf{0}} ; st_1 := \circ W_{\mathbf{0}} ;$ 
  when b       $\Rightarrow \pi_0 := b-2 ; \pi_1 := b-1 ;$ 
                 $w_0 := 10 ; w_1 := 11 ;$ 
                 $st_0 := \circ W_{\mathbf{0}} ; st_1 := \circ B_{\mathbf{0}} ;$ 
end case ;
 $\pi_2 := \pi_1 ; w_2 := w_1 ; st_2 := st_1 ;$ 
while w  $\neq \emptyset$ 
loop d := pop(w) ;
  ( $f_0, f_1, f_2, c, nst_0, nst_1, nst_2$ ) := select( $w_0, w_1, w_2, d, st_0, st_1, st_2$ ) ;
   $\pi_0 := \pi_{f_0} \& \{c\} ; w_0 := w_{f_0}.d ;$ 
  if  $f_1 = f_0$  then  $\pi_1 := \pi_{f_0} \& \{c+1\} ; w_1 := w_{f_0}.\mathcal{A}(d+1) ;$ 
  else  $\pi_1 := \pi_{f_1} \& \{0\} ; w_1 := w_{f_1}.first(top(st_{f_1})) ;$ 
  end if ;
  if  $f_2 = f_1 = f_0$  then  $\pi_2 := \pi_{f_2} \& \{c+2\} ; w_2 := w_{f_0}.\mathcal{A}(d+2) ;$ 
  else if  $f_2 = f_1$  then  $\pi_2 := \pi_{f_1} \& \{1\} ;$ 
                 $w_2 := w_{f_1}.second(top(st_{f_1})) ;$ 
  else  $\pi_2 := \pi_{f_2} \& \{0\} ; w_2 := w_{f_2}.first(top(st_{f_2})) ;$ 
  end if ;
  end if ;
end loop ;
output :  $\pi_0, w_0, st_0 ;$ 

```

**Figure 14** The linear algorithm for the path to the root. Recall that  $\mathcal{A}(n)$  is the coordinate of  $n$ .

At last, the selection of three digits at each step insures the continuity of the path and that the last node which will be found at the end of the computation is the node whose coordinate was given as an input.

Now, consider the coordinates of the father. The path from the root to the node is associated with the list of the statuses of the nodes belonging to the tree. As the father is the penultimate node on the path, its status is the penultimate element of the list. Now, from the status and the last digits of the coordinates of the nodes, it is possible to compute the coordinate of the father. Let  $\nu a$  be the coordinate of the node. For nodes for which the preferred son property is

true, the coordinate of the father is  $\nu$  or  $\mathcal{A}(\nu-1)$  depending on  $a$  and on the patterns of the node. The preferred son property is not true for the nodes with the status  $\circ W_0$  in 0, *i.e.* which ends in an odd number of 0's and for the nodes with the status  $\mathbf{2}W_2$ . For the first case, the penultimate digit of the node is  $b_1$  or  $b$ . Erasing the last digit gives  $\nu_1 b_1$  or  $\nu_1 b$ . Now,  $\mathcal{A}(\nu_1 b) = \nu 0$  and in the other case, we append 1 to  $\nu_1 b_1$  and again we use  $\mathcal{A}$ . For a node in  $\mathbf{2}W_2$ , the computation is easy: we erase the last digit  $\alpha_0$  and append 1 or 2, depending on  $\alpha_0$ . For nodes with the same status ending in 00, we apply a similar argument as we obtain  $\nu_1 b_2$  or  $\nu_1 b_1$  after erasing  $\alpha_0$ .

We remain with the problem of finding the other neighbours of the node in the tiling. As the solution of this question is tightly connected with the construction of the dual graph of the tiling, we postpone this part after the statement of theorem 6. The result will be completely proved when the discussion about the dual graph will be completed.

Up to the last neighbours which we have still to characterize, we proved the following result:

**Theorem 6** *For each tiling  $\{p, q\}$ , when  $p > 3$ , there is an algorithm linear in the coordinate of a node  $\nu$  in order to compute the path from the root to  $\nu$ , to compute the status of the node, the coordinate and the status of its father and, more generally of its sons in the tree and among them, which are its neighbours in the tiling.*

What remains to prove of theorem 6 is connected with the dual graph of the tiling and it will give us an algorithmic way to determine the dual graph by placing the **missing** arcs which will transform the tree of the splitting into the restriction of the dual graph to the considered region.

First, let us formulate a general remark. Consider a region  $R$  with its leading tile  $T$ . The splitting gives us in one round several regions whose leading tiles are not neighbours of  $T$ . This means that only a few nodes among the sons of  $T$  are its neighbours in the tiling. The second remark is that there are also other nodes which are not on the same level which are also neighbours of  $T$ : this is the case, for instance, when the father of a node is also one of its neighbours. We shall see that this observation is general. The fact that we have several tiles around a tile in one round entails that the standard representation of the tree with horizontal levels has a cost: as we shall see, it entails a distortion with the neighbours of certain kinds of nodes.

Secondly, let us make another remark about the splitting. As can easily be seen from figures 6 up to 9, several regions defined by the splitting of  $R$  share a vertex of  $T$ . Let us call a **chain** a maximal subset of the sons of  $T$  such that the corresponding leading tiles share the same vertex of  $T$ . Up to now, we did not make it completely exact how the sons of the tree are displayed. Taking again

figures 6 up to 9, we consider that the sons of a node are given in the following way, also see figure 15 below, which zooms at figures 8 and 9.

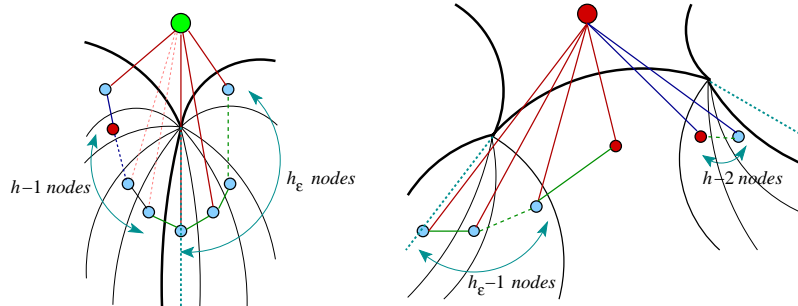


**Figure 15** Zooming on figures 8 and 9. Note the counting of the nodes which belong to a chain.

On the left-hand side: the chain around an ordinary vertex: between two regions which are copies of  $S_0$ . The main leading tile may be a white or a black node.

On the right-hand side: the chain around the vertices shared by the leading tile of a copy of  $D_1$ . The main leading tile is a black node.

For a white node  $\nu$ , going from the left to the right we have  $p-3$  chains, each one containing  $h_\epsilon$  nodes,  $\epsilon$  depending on the parity, as defined previously. Each chain is displayed in this way: this time from the right to the left, we have the son of  $\nu$  which shares a side with  $\nu$ : it is a neighbour of  $\nu$ ; next we have nodes of the chain which share a side with the following node of the chain, except for the last one of the chain. Call this last node of the chain an **end-node** son of  $\nu$ . The node of the chain which is a neighbour of  $\nu$ , in the display, it is the rightmost node of the chain, is called a **marked** son of  $\nu$ . The other white sons of  $\nu$  are called **ordinary** sons and they are not neighbours of  $\nu$ .

It is not difficult to characterize these different kinds of nodes among the sons of  $\nu$ . It is rather easy to compute them from the status of  $\nu$  and the characteristics of its sons. As an example, let us explain this computation on a white node with the status  $\circ W_\circ$ . Then,  $\nu$  has  $p-2$  neighbours among its sons. Their characteristics have the form  $1+j.h_\epsilon$  with  $j \in \{1..p-4\}$ , or 0 or 1. Indeed, 1 is the characteristic of the black son of  $\nu$  which is a neighbour. From the display which we adopted, 0 is the first node of a chain and so, it is also a neighbour of  $\nu$ . We easily check that  $b = 1+(p-3)h_\epsilon$  which explains the above characterization of the marked sons of  $\nu$ . For white nodes with other statuses, we have a different situation.

For a black node  $\nu$ , the computation is similar up to the following difference. In the splitting defined by figures 6 up to 9, the black son of  $\nu$  is no more the rightmost one: also see figure 15. The rightmost sons are white and they belong to



a chain which is displayed in another direction: the marked son which starts the chain is the right-hand neighbour of the black son of  $\nu$  and the successive nodes of the chain are displayed from the left to the right and the end-node of this chain is the rightmost son of  $\nu$ . On the left-hand side of the black son of  $\nu$ , the display is exactly the same as for a white node. There is still a difference in the number of nodes in a chain: the leftmost chains contain  $h_\epsilon - 1$  nodes, the rightmost chain contains  $h - 2$  nodes and the other chains contain each one  $h_\epsilon$  nodes, see figures 6 up to 9. As an example, the marked sons of a black node of status  $\circ B \circ$  which ends in 0 have the following characteristics:  $j h_\epsilon$  for  $j \in \{1..p-3\}$ , or 0 or 1.

Below, table 4 gives the form of marked sons of a node for all possible configurations.

At this point, as the computations of the characteristics and the matrix of the splitting indicates, we remark that we have all the neighbours of a black node. Indeed, we know that a black node is always a neighbour of its father and table 4 indicates that a black node has  $p-1$  marked sons. Accordingly, all the neighbours of a black node are known and the proof of theorem 6 is complete for this case.

We remain with the neighbours of a white node  $\nu$ . Let  $\mu$  denote the father of  $\nu$ . If  $\nu$  is an ordinary son of  $\mu$ , it is in a chain. As it is not a marked son, it is not the first element of the chain. As it is not an end-node it is not the last. Accordingly, it has a left-hand neighbour in the chain and also a right-hand one. If  $a$  is the characteristic of  $\nu$  and if  $\nu$  is written  $\nu_1 a$ , then the just indicated nodes have  $\nu_1 a_1$  and  $\nu_1 a'$  as coordinates where  $a = a_1 + 1$  and  $a' = a + 1$ . We may have to compute the predecessor of  $\nu_1$  when  $a = 0$ ,  $a = k_1$  or  $a = b_1$ . This computation is linear in  $\nu_1$ . And so, in this case we have the missing neighbours and the theorem is proved for ordinary white sons of a node.

The case of marked nodes is also simple. One neighbour is the father, the other is the left-hand neighbour on the chain which is started by the marked node. If  $\nu$  is the coordinate of the marked node, the above algorithm allows us to compute the coordinate of the father, and the coordinate of the other neighbour is  $\mathcal{A}(\nu - 1)$ .

And so, we remain with the case of an end-node of a chain.

We have three cases: the leftmost son of a node, the rightmost son of a black node and the other end-nodes among the sons.

Let us start with an end-node  $\nu$  which is neither the leftmost son nor the rightmost son of the father  $\mu$  of  $\nu$ .

There are  $2h_\epsilon + 2 - \epsilon$  tiles around a vertex. Let  $V$  be the vertex which belongs to all nodes of the chain of which  $\nu$  is an end-node. Of course,  $\mu$  shares  $V$  also, by definition of a chain. With the members of the considered chain, we have  $h_\epsilon + 1$  nodes. We still need  $h_\epsilon + 1 - \epsilon = h$  nodes, which no more depends on the parity of  $q$ . We obtain these nodes as follows: let  $\varpi$  be the son of  $\mu$  which is on the

left-hand of  $\nu$ . We know that  $\varpi$  is a marked son. Looking at figures 6 up to 9, we see that the expected nodes are on the chain to the right which comes from the black son of  $\varpi$  which is also the rightmost son of  $\varpi$  as  $\varpi$  is a white node. The chain has  $h-2$  nodes. Adding  $\varpi$  and its black son, we have the required number of nodes. It is not difficult to see that all these nodes have  $V$  as a vertex and so we have the expected nodes. As we know the father of  $\nu$  from the above algorithm, we also have  $\varpi$  which is a son of  $\mu$  and, unfolding the loop of the algorithm for two more steps, we get the coordinates of the black son  $\varphi$  of  $\varpi$  and of the rightmost son  $\vartheta$  of  $\varphi$ .

Now, let us turn to the case of the leftmost and rightmost sons of a node.

In order to handle these situations, first we look at another problem which we already met: define an **elementary cycle** of the dual graph of the splitting to be the set of all the tiles which share a common vertex. We shall distinguish between **within-tree** and **inter-tree** cycles. Within-tree cycles are illustrated, below, by figure 16 both in the case of a white node and of a black node. We can see from the figure that all cases of within-tree cycles are indicated by the black node case. Inter-tree cycles can be obtained by looking at how we continue with within-tree cycles. When nodes are neighbours of the next one, we have again ordinary cycles which we shall define a bit later. Now, the connections between subtrees are the same as between trees. This is why this continuation gives us the required information which is displayed by figure 17. Both pictures of the latter figure show up a new type of cycle which we call **inter-leave** cycle.

Now, we describe these configurations.

There are five configurations for an elementary cycle, four of them are within-tree and the last one is inter-tree.

An **ordinary** cycle is defined by two consecutive nodes in a chain, say  $\varpi$  and  $\mu$ . It consists of  $\varpi$ ,  $\mu$ , the leftmost chain of sons of  $\mu$  and the rightmost chain of sons of  $\vartheta$ , the rightmost son of  $\varpi$ . This gives us  $1 + 1 + h_\epsilon + h - 2 + 1 = 2h + \epsilon$  nodes, as  $h_\epsilon = h - 1 + \epsilon$ . As  $\epsilon$  is 0 when  $q$  is even and 1 when it is odd, we have the right number of nodes.

A second configuration is characterized by  $\varpi$  and  $\mu$  being again consecutive white nodes but  $\varpi$  is the first node of a chain  $\kappa$  and  $\mu$  is the end-node of the chain which is on the right-hand side of  $\kappa$ . In this case,  $\varpi$  and  $\mu$  have the same father  $\omega$  and so, the cycle consists of  $\omega$ , the chain of sons of  $\omega$  with  $\mu$  as its end-node, the rightmost chain of  $\vartheta$ , the rightmost son of  $\varpi$  together with  $\vartheta$  and  $\varpi$ . We again have  $1 + h_\epsilon + h - 2 + 1 + 1 = 2h + \epsilon$  nodes, which is the required number. Call such a configuration **end-point**.

A third configuration is characterised by two consecutive nodes,  $\varpi$  and  $\mu$  which have the same father  $\omega$ , with  $\varpi$  white and  $\mu$  black,  $\mu$  being on the right-hand side of  $\varpi$ . The cycle is then defined by  $\omega$ ,  $\mu$ , its leftmost chain, the rightmost chain of  $\vartheta$ , the rightmost son of  $\varpi$ ,  $\vartheta$  and  $\varpi$ . The counting is  $1 + 1 + h_\epsilon - 1 +$

$h-2 + 1 + 1 = 2h+\epsilon$ , as required. Call such a configuration **left-hand black**.

The fourth configuration is **right-hand black**: it is defined by two consecutive nodes,  $\varpi$  and  $\mu$  with the same father  $\omega$  and  $\mu$  on the right-hand side of  $\varpi$ . But, this time,  $\varpi$  is black and  $\mu$  is white. The cycle consists of  $\omega$ ,  $\mu$ , the leftmost chain of sons of  $\mu$ , the rightmost chain of sons of  $\varpi$  and  $\omega$ . The counting is  $1 + 1 + h_\epsilon + h-2 + 1 = 2h+\epsilon$ , as required.

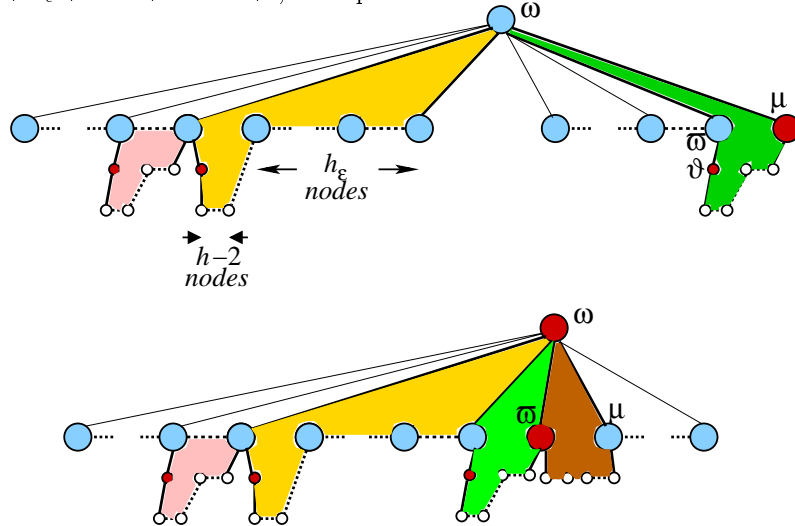


**Figure 16** The configurations of elementary cycles of the dual graph.

From the left to the right, on the lower picture:

ordinary cycle, end-node cycle, left-hand black cycle, right-hand black cycle.

Note the indication of the number of nodes in an end-node cycle. The same counting holds for the ordinary cycles.

Consider the sub-trees of the tree rooted in  $\nu$  which are rooted in the sons of  $\nu$ . The four within-tree configurations can also be viewed as the starting point of inter-tree cycles by only considering the leftmost and rightmost nodes of each level of the sub-trees. This is done in figure 17 for the ordinary and the end-node cycles, and it appears that the continuation gives always rise to the same type of cycle which we call **inter-leave**. Strictly speaking, there are infinitely many patterns of inter-leave cycles. However, they can be described by a single rule. An inter-leave cycle is defined by two white nodes  $\mu$  and  $\varpi$ . The node  $\mu$  is the leftmost node of its level in a sub-tree  $\mathcal{B}$  and  $\varpi$  is a rightmost node of **another deeper level**, of the neighbouring sub-tree of  $\mathcal{B}$ ,  $\mathcal{C}$ . We consider that the roots of  $\mathcal{B}$  and  $\mathcal{C}$  are consecutive nodes on some level of the spanning tree. Let  $\ell$  be the difference between the level of  $\mu$  and the level of  $\varpi$ . Then, let  $\nu$  be the leftmost son of  $\mu$ . Then the rightmost son of  $\varpi$  is a black node which, consequently, cannot share a side with a node which does not belong to  $\mathcal{C}$ . Let  $\vartheta$

be the rightmost son of the black son of  $\varpi$ . Then  $\vartheta$  is a white node, and a simple counting argument shows that we have a new inter-leave cycle which consists of  $\varpi$ ,  $\mu$ , the leftmost chain of  $\mu$  which ends in  $\nu$ , the black son of  $\varpi$  and the rightmost chain of this black node which ends in  $\vartheta$ . Now, the difference of levels between  $\nu$  and  $\vartheta$  is  $\ell+2$ . And so, measured from the original level of the roots of the subtrees, the depth of the bottommost node of an inter-leave cycle is twice the depth of its upmost node.

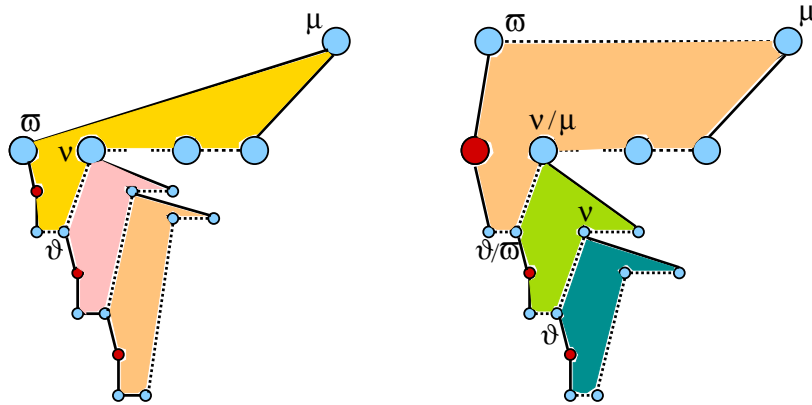


**Figure 17** *The continuation of end-node and ordinary cycles. Note the increasing in the distance between the closing nodes.*

This remark shows that the algorithm described above is still linear in this case: we have to repeat the body of the loop until  $\vartheta$  is found. This can be performed without counting: when the node  $\nu$  is reached, we repeat again the path starting from the root in order to find the point starting from which all the nodes down to  $\nu$  are leftmost nodes of their level. As we know the status at each step of the process this raises no problem. Starting from the first leftmost node on the path, we compute the other path, each step requires a constant time, and we go down two steps on the new path when we go down by one step on the path to  $\nu$ . This way,  $\vartheta$  is reached when  $\nu$  is reached.

Now, we can see that this situation is general for inter-tree cycles. Indeed, call **closing** nodes the rightmost son  $\vartheta$  of a black node which is the neighbour of the leftmost son  $\nu$  of a white node such that the grandfather of  $\vartheta$  shares a side with an **ancestor** of  $\nu$ . Then, from the closing nodes of an inter-tree cycle, as shown by figure 16, we can construct another inter-tree cycle, and so this generates an infinite sequence of inter-tree cycles. Figure 17 shows that the closing nodes of an end-node cycle or an ordinary cycle are the starting point of an inter-tree cycle. Now, the configuration of left- and right-hand black cycles allow us to

construct inter-tree cycles: this is clear for the closing nodes of a left-hand black cycle. For a right-hand black cycle, the closing nodes are the starting nodes of an ordinary cycle and the closing nodes of this ordinary cycle start an infinite sequence of growing inter-tree cycles.

Note that we have in fact two left-hand black cycles: one where the top node is white, the other where it is black.

config.	$\chi$ 's for the sons	marked sons
$\circ W_{\circ}$	$2 \dots b_1 0 1$	$1 + jh_{\epsilon}, 0, 1, j \in \{1..p-4\}$
$1 W_1$	$k'' \dots b_1 0 \dots k'$	$k' + jh_{\epsilon}, k, k', j \in \{1..p-4\}$
$2 W_2$	$\alpha'' \dots b_1 0 \dots \alpha'$	$3 + \epsilon + jh_{\epsilon}, \alpha', j \in \{0..p-4\}$
$1 W_{\circ}$	$k'' \dots b_1 0 \dots k_1 0 1$	$k' + jh_{\epsilon}, 0, 1, j \in \{1..p-4\}$
$\circ W_2$	$2 \dots k_1 0 \dots \alpha'$	$3 + \epsilon + jh_{\epsilon}, \alpha', j \in \{0..p-4\}$
$\circ B_{\circ} 1$	$2 \dots k_1 0 \dots b_1 0 1$	$2 + \epsilon + jh_{\epsilon}, \alpha, \alpha', j \in \{0..p-4\}$
$\circ B_{\circ} 0$	$2 \dots b_1 0 \dots k_1 0 1$	$jh_{\epsilon}, 0, 1, j \in \{1..p-3\}$
$2 B_{\circ}$	$\alpha'' \dots b_1 0 \dots b_1 0 1$	$jh_{\epsilon}, 0, 1, j \in \{1..p-3\}$
$\circ B_1$	$2 \dots b_1 0 \dots k'$	$jh_{\epsilon}, 0, 1, j \in \{1..p-3\}$

**Table 4** *The marked sons of a node: the neighbours among the sons.*

situation of $\nu$	non-son neighbours
leftmost son	$\nu+1, \rho^{\ell}(\nu-1)$
rightmost son	$\nu-1, f^{\ell}(\nu+1)$
end-node	$\nu+1, \rho^{\ell}(\nu-1)$
marked, left-hand of black son	$\nu-1, f(\nu)$
marked, right-hand of black son	$f(\nu), \nu+1$
ordinary	$\nu-1, \nu+1$

**Table 5** *The neighbours of a white node not among the sons.*

With this study the proof of theorem 6 is completed for what is the general case. We collect the information about the neighbours in table 5, above. Note that table 5 makes use of two auxiliary functions:  $f(\nu)$  denotes the coordinate of the father of  $\nu$  and  $\rho(\nu)$  denotes the rightmost son of  $\nu$ .

It remains to prove that theorem 6 is also true for the particular cases. Remind that in these cases, the preferred son property is true. Accordingly, finding the coordinates of the father is very easy. For the path from the root to the node, it is enough to repeat the same algorithm but this time, things are much simpler as the reader may easily realize.

## 7 Conclusion

Theorem 6 completely answers a complexity question about the tilings  $\{p, q\}$ . This indicates that if we wish to implement cellular automata on such tilings, it is in principle easily feasible thanks to the construction of the algorithms of section 5.

However, the situation is not always this one in tilings of hyperbolic spaces. In dimensions 3 and 4, it seems that we have not such efficient algorithms. First, note that when we speak about tilings constructed by tessellation, we have only finitely many ones in dimensions higher than 2. There are four such tilings in the hyperbolic 3D space and five of them in the hyperbolic 4D space. Starting from dimension 5, there are no such tilings, see [Sommerville 1958].

But the hyperbolic plane gives us infinitely many tilings in which the tilings  $\{p, q\}$  certainly constitute a small family. It is certainly interesting to investigate which families consist of combinatoric tilings. This is a broad field completely open.

## Acknowledgement

The author is very much in debt to the anonymous referee for remarks which helped him to make the paper better readable.

## References

- [De la Harpe et al. 1990] Sur les groupes hyperboliques d'après Michael Gromov, E. Ghys, P. de la Harpe (ed.), Progress in Mathematics, **83**, Birkhäuser, (1990).
- [Margenstern et al. 2004a] Chelghoum K., Margenstern M., Martin B., Pecci I.: Cellular automata in the hyperbolic plane: proposal for a new environment, *Lecture Notes in Computer Sciences*, **3305**, 2004, 678-687, proceedings of **ACRI'2004**, Amsterdam, October, 25-27, 2004.
- [Margenstern et al. 2004b] Chelghoum K., Margenstern M., Martin B., Pecci I., Skořdev G.: Tilings  $\{p, q\}$  of the hyperbolic plane are combinatoric, **WTCA'2004**, *International Workshop on Tilings and Cellular Automata*, in **DLT'04**, Auckland, New-Zealand (Aotearoa), December, 12, 2004, Proceedings of WTCA, 2004, CDMTCS **253**, Research Report Series.

- [Fraenkel 1985] Fraenkel, A. S.: Systems of numerations, *American Mathematical Monthly*, **92**, 1985, 105–114.
- [Hollander 1998] Hollander, M.: Greedy numeration systems and regularity, *Theory of Computing Systems*, **31**, 1998, 111–133.
- [Lothaire 2002] M. Lothaire, Algebraic combinatorics on words, Cambridge University Press, 2002.
- [Margenstern 2002a] Margenstern, M.: A contribution of computer science to the combinatorial approach to hyperbolic geometry, **SCI'2002**, Orlando, USA, July, 14-19, (2002), vol. 5, 423-428, ISBN 980-07-8150-1.
- [Margenstern 2001] Margenstern, M.: New tools for cellular automata in the hyperbolic plane, *Journal of Universal Computer Science*, **6**(12), 2000, 1226–1252.
- [Margenstern 2002] Margenstern M.: The splitting method and Poincaré's theorem: (I) – the geometric part, *Computer Science Journal of Moldova*, **10**(3), 2002, 297-319.
- [Margenstern 2003a] Margenstern, M.: Revisiting Poincaré's theorem with the splitting method, **Bolyai'200**, *International Conference on Geometry and Topology*, Cluj-Napoca, Romania, October, 1-3, 2002, (2003), 81-108, Cluj, University Press, ISBN 973-610-205-X.
- [Margenstern 2003b] Margenstern M.: Implementing Cellular Automata on the Triangular Grids of the Hyperbolic Plane for New Simulation Tools, *Proceedings of ASTC'2003*, March, 29 – April, 4, 2003, Orlando, Florida, USA.
- [Margenstern 2003c] Margenstern M.: The splitting method and Poincaré's theorem: (II) – matrix, polynomial and language, *Computer Science Journal of Moldova*, **11**(1), 2002, 3-27.
- [Margenstern 2003d] Margenstern, M.: On the Infinigons of the Hyperbolic Plane, A combinatorial approach, *Fundamenta Informaticae*, **56**(3), 2003, 255–272.
- [Margenstern 2004] Margenstern, M.: The tiling of the hyperbolic 4D space by the 120-cell is combinatoric, *Journal of Universal Computer Science*, **10**(9), 2004, 1212-1238.
- [Margenstern and Morita 2001] Margenstern, M., Morita K.: NP problems are tractable in the space of cellular automata in the hyperbolic plane, *Theoretical Computer Science*, **259**, 2001, 99–128.
- [Margenstern and Skordev 2003a] Margenstern M., Skordev G., The tilings  $\{p, q\}$  of the hyperbolic plane are combinatoric, "Proceedings of **SCI'2003**, July 27-30, Orlando, Florida, USA".
- [Margenstern and Skordev 2003b] Margenstern, M., Skordev, G.: Fibonacci Type Coding for the Regular Rectangular Tilings of the Hyperbolic Plane, *Journal of Universal Computer Science*, **9**(5), 2003, 398–422.
- [Margenstern and Skordev 2003c] Margenstern, M., Skordev, G.: Tools for devising cellular automata in the hyperbolic 3D space, *Fundamenta Informaticae*, **58**(2), 2003, 369–398.
- [Meschkowski 1964] H. Meschkowski, *Noneuclidean Geometry*, translated by A. Shenitzer. Academic Acad. Press, NY, 1964.
- [Poincaré 1882] Poincaré H., Théorie des groupes fuchsien. *Acta Mathematica*, **1**, 1–62, (1882).
- [Sommerville 1958] Sommerville, D.: *An introduction to the geometry of N dimensions*, Dover Publ. Inc., New-York, 1958.